DIPLOMARBEIT

Titel der Diplomarbeit

„Locally rotationally symmetric Bianchi type I cosmological models with anisotropic matter sources“

Verfasserin

Bettina Wutzl, Bakk.rer.nat. BSc

angestrebter akademischer Grad

Magistra der Naturwissenschaften (Mag.rer.nat.)

Wien, 2013

Studienkennzahl lt. Studienblatt:	A 411
Studienrichtung lt. Studienblatt:	Diplomstudium Physik
Betreuerin / Betreuer:	MMag. Dr. Johannes Markus Heinzle

Contents

Convention

Throughout this thesis the convention 8πG=1 and c=1 is used. Moreover we will use *Einstein summation convention.*
The range of Greek indices is $0, 1, 2, 3$ alternatively we use t, x, y, z. Latin indices, on the other hand, take the values $1, 2, 3$.

Abstract

In this thesis we examine dynamics of cosmological models with anisotropic matter. We consider spatially homogeneous local rotationally symmetric models of Bianchi type I. The anisotropic matter models used are the ones developed by Calogero and Heinzle [4] which generalise perfect fluids and include elastic matter, collisionless matter as well as magnetic fields. Solutions of the Einstein equations for such models are generated by employing the dynamical system approach where the emphasis lies on approximation techniques. Several solutions (also including Kasner and FLRW solutions) are investigated as to their observational relevance and in view of their consistence with observations from which the age of the universe is inferred. In particular we analyse isotropization of anisotropic models towards the isotropic FLRW cosmological model. It is shown that models with a small anisotropy parameter exhibit a similar behaviour as perfect fluids. Moreover drawbacks and possibilities for improvement of the given model are discussed.

Zusammenfassung (German abstract)

In dieser Diplomarbeit untersuchen wir die Dynamik von kosmologischen Modellen mit anisotropischer Materie. Wir nehmen räumlich homogene rotationssymmetrische Modelle vom Bianchi Typ I an. Die verwendeten anisotropischen Materiemodelle sind die, welche von Calgero und Heinzle entwickelt wurden [4] und welche perfekte Flüssigkeiten generalisieren und sowohl elastische Materie, kollisionsfreie Materie als auch magnetische Felder enthalten. Lösungen der Einstein-Gleichungen für solche Modelle werden erstellt unter der Verwendung des Zugangs über dynamische Systeme, wo der Schwerpunkt auf Approximationsmethoden liegt. Verschiedene Lösungen (auch die Kasner- und FLRW-Lösung) werden untersucht auf ihre beobachtbare Relevanz und in Hinblick auf die Konsistenz mit Beobachtungen, aus welchen das Alter des Universums abgeleitet wird. Im Speziellen analysieren wir die Isotropisierung von anisotropen Modellen zum isotropischen FLRW-kosmologischen Modell. Es wird gezeigt, dass Modelle mit kleinen anisotropischen Parametern ein ähnliches Verhalten zeigen wie perfekte Flüssigkeiten. Weiters werden Schwächen und Verbesserungsmöglichkeiten des Modells angegeben.

1 Introduction

In the late 17^{th} century one of the greatest physicists *Sir Isaac Newton* (1642-1727) revolutionised physics with his work *Philosophiæ Naturalis Principia Mathematica* [21] (in general referred to as Principia). He was the first to describe the phenomenon which he called *gravitation*. In his works he introduced three main laws of physics of which his second law says that force is proportional to mass. Newton defined the term *inertial frame*. An inertial frame is a frame in which the physical laws (as he described them) hold. To transform an inertial frame into another inertial frame elements of the *Galileo group* are used. The Galileo group is a group of transformations that leave the equations of motion invariant. Newton describes the inertial frames in his Principia via *absolute space* [22] p.77.

> Absolute space, in its own nature, without regard to anything external, remains always similar and immovable. Relative space is some movable dimension or measure of the absolute spaces ; which our senses determine by its position to bodies ; and which is vulgarly taken for immovable space ; such is the dimension of a subterraneous, an æreal, or celestial space, determined by its position in respect of the earth. Absolute and relative space, are the same in figure and magnitude ; but they do not remain always numerically the same.

The construct of an *absolute space* was discussed and criticised by a lot of people. One of the most famous counterparts was Gottfried Wilhelm Leibniz (1646-1716). Leibniz discussed a lot (among others about the construct of an absolute space) with Samuel Clarke (1675-1729), who defended Newton. In his fifth letter to Clarke Leibniz wrote [7] p.181:

> I have demonstrated, that *Space* is nothing else but an *Order* of the existence of things, observed as existing Together; And therefore the Fiction of a material finite Universe, moving forward in an infinite empty Space, * cannot be admitted.* It is altogether unreasonable and *impracticable*. For, besides that there is *no real Space* out of the material Universe;

The most of the critics gave just philosophical reasons for the not existence of the absolute space. The first to specify his critique physically was Ernst March (1836-1916) [15] p.232.

> Newton's experiment with the rotating vessel of water simply informs us, that the relative rotation of the water with respect to the sides of the vessel produces no noticeable centrifugal forces, but that such forces are produced by its relative rotation with respect to the mass of the earth and the other celestial bodies. No one is competent to say how the experiment would turn out if the sides of the vessel increased in thickness and mass till they were ultimately several leagues thick. The one experiment only lies before us, and our business is, to bring it into accord with the other facts known to us, and not with the arbitrary fictions of our imagination.

Mach's principle says that "the mass of the Earth and the other celestial bodies" influence the environment and that this influence determines Newton's inertial frames.
The next who broke the principle of Galilean relativity (meaning that physical laws stay equal under Galilean transformations) was James Clark Maxwell (1831-1879). He introduced a theory of electrodynamics in 1864. As a consequence of this theory follows that the speed of light in vacuum is constant. This universal constant breaks the concept of Galilean transformation. In the years of Maxwell it was believed that there was some medium called *ether* which carries electromagnetic waves such as light. Hence it was thought that Maxwell's equation hold only in such frames which are in rest with respect to the ether. A lot of experiments were constructed to prove the existence of the *ether*. Without doubt the most popular one is the *Michelson-Morley experiment* of 1887 [20]. However none of these experiments were able to find even the smallest trace of this ether.

Finally Albert Einstein (1879-1955) was the one to set an end to the pointless search for this invisible medium which was thought to be a carrier of light. He replaced the Galilean transformations with new transformations called *Lorentz transformations*. This different group of transformations leave Maxwell's equations (and thus the constant speed of light) invariant but they do not leave Newton's equation unaltered. It is because of this that Einstein had to develop some new equations of motion. This resulted in the *Special Theory of Relativity*.

In the relativistic view of physics what was still missing was a corresponding theory of gravitation. A huge step in relativistic physics was made in 1907 when Einstein stated the equivalence of gravitation and inertia [9]. In the following years Einstein cooperated with several physicists and mathematicians, like Abraham, Nordström or Grossman. After years of productive cooperation the *General Theory of Relativity* [8] was published by Einstein in 1916. That theory is described by a set of differential equations, the *Einstein equations*. Since these equations have been published several scientists have tried to solve them. Einstein himself was very distraught by his equations because he could not find a solution describing a static universe. He was convinced that the universe has to be static thus he added a cosmological constant to his equations to gain such a static solution. History tells us that later Einstein removed the cosmological constant because of Hubble's observations of which was concluded that the universe expanded. It is said that from then on he just referred to the cosmological constant as "the greatest blunder of my[his] life".
Nowadays there are big discussions whether the removal of the cosmological constant was a "blunder" or not. This will be discussed in more detail in the last section.

The first to introduce an expanding universe were Alexander Friedmann (1888-1925) and Georges Edouard Lemaître (1894-1966) in the 1920s which coincides with the results of Hubble's observations. Once introduced Howard Percy Robertson (1903-1961) and Arthur Geoffrey Walker (1909-2001) gave a geometric foundation to the expanding spatially homogeneous and isotropic universe model of Friedmann and Lemaître. Thus this model is often referred to as FLRW model. Since this model is of fundamental significance we will also discuss it, namely theoretically in section 4.3 and as to its observational relevance in section 6.3.

The FLRW model, which is a indeed very special model, is inaccurate because obviously the universe is not spatially homogeneous, at least not on all scales. This drawback entailed the search for more general solutions of the Einstein equations. The first idea was to use perturbation theory to get more general results. This approach gave in fact information about the space of general models but just in the environment of the FLRW models which was unsatisfactory since perturbation theory fails when trying to delineate the nonlinear comportment of the Einstein equations. Since a method to describe inhomogeneous and anisotropic models was needed the employment of dynamical systems theory, which was fathered by Henri Poincaré (1854-1912) and advanced by George David Birkhoff (1884-1944), started in theoretical cosmology. Dynamical systems describe how physical systems develop in time. We will also use the theory of dynamical systems to find solutions of the Einstein equations for our matter model thus we will give a brief introduction to this topic in the following section 2.

After having given the mathematical basis which is needed to understand this thesis section 3 serves as introduction to the physical problem. In general one will not find any solutions of the Einstein equations without making restrictions. The main results to date make use of a spatially homogeneous spacetime. The first to classify different types of models with spatially homogeneous spacetime was Luigi Bianchi (1856-1928) after whom the models are named nowadays. Then, in the 1960s, Engelbert Schücking (*1926) and Christoph G. Behr enhanced and completed Bianchi's classification. The Bianchi models are used frequently and form a focal point in modern general relativistic research. In this thesis we will only examine the most basic one which is the Bianchi type I model. In section 4 we search for solutions of the Einstein equations for locally rotationally symmetric (LRS) Bianchi type I models with a perfect fluid source. Such a model contains the mentioned FLRW solution as well as the Kasner solution (i.e. a solution for a vacuum model which is special type of perfect fluid.

The next ambition in this thesis is to find even more general solutions. Thus in section 5 we consider anisotropic matter models. The anisotropic matter models we use are the ones which have been developed by Calgero and Heinzle [4] and which generalise perfect fluids. In this section we will use the theory of dynamical systems, summarized in section 2, to generate solutions.

Found theoretical results it is advisable to check for its experimental accordance. That is what section 6 serves for. Since the fundamental observations of Hubble enormous progress has been made. We will discuss some of the most important attainments of observational astronomy. Moreover we will compare them to our theoretical results of the earlier sections and see whether they are in agreement or not. The focus lies on the estimation of the age of the universe. Hence we will compare the age gained from observational data to the age we achieve using theoretical considerations.

The ending of this thesis form section 7 which gives an insight into the discussion whether the cosmological constant is zero or not. Moreover we will present drawbacks and possibilities of improvement of our model.

2 Dynamical System

In this section we will introduce some basics of the theory of dynamical systems which we will need for our calculations later. Since this section serves only as basis for the following we will not prove any of the lemmas or theorems given.

Dynamical Systems use specific rules to closely examine the change of behaviour of a point in certain geometrical space with time. There are a lot of applications of such systems in mathematics, physics and biology. The simplest example of a dynamical system is an ordinary differential equation.

We will examine dynamical systems of the form

$$\dot{x} = f(x) \tag{1}$$

with a C^1 vector field $f : \mathbb{R}^n \to \mathbb{R}^n$ and a function $x : \mathbb{R} \to \mathbb{R}^n$.

2.1 Qualitative analysis

2.1.1 Systems of linear and autonomous equations

The presentation given below follows the one given in [30] p.180 ff.

In this section we consider systems of the form

$$\dot{x} = Ax \tag{2}$$

with $x = x(t) \in \mathbb{R}^n$ and a matrix with constant coefficients $A \in \mathbb{R}^{n \times n}$.

To solve (2) *Jordan normal form* will be needed. A matrix in Jordan normal form looks like (k is the number of different blocks)

$$J = \begin{pmatrix} J_1 & & & \\ & J_2 & & \\ & & \ddots & \\ & & & J_k \end{pmatrix}, \tag{3}$$

with J_i being a matrix of the size $r_i \times r_i$. These J_i are of the form

$$J_i = \begin{pmatrix} \lambda_i & 1 & 0 & \dots & 0 \\ 0 & \lambda_i & 1 & \dots & 0 \\ \vdots & \vdots & \ddots & \ddots & \vdots \\ 0 & \dots & \ddots & \lambda_i & 1 \\ 0 & \dots & \dots & 0 & \lambda_i \end{pmatrix}.$$

The λ_i are eigenvalues of the matrix A. Each block has just one eigenvalue. We know from Linear Algebra that there is a nonsingular matrix C for every matrix A so that

$$J = C^{-1}AC$$

with J being a matrix in Jordan normal form. We can use this to transform equation (2) via

$$x = Cy \qquad\qquad y = C^{-1}x$$

and get

$$\dot{y} = Jy \qquad \text{with} \qquad J = C^{-1}AC. \tag{4}$$

This transformation gives a decoupled system of differential equations which can be solved. There is a fundamental matrix for each Jordan block. The associated fundamental matrix of J is $(Y(0) = I)$

$$Y(t) = \begin{pmatrix} Y_1 & & & \\ & Y_2 & & \\ & & \ddots & \\ & & & Y_k \end{pmatrix}$$

with Y_i being of the form (r_i is the size of the Jordan block)

$$Y_i(t) = \begin{pmatrix} e^{\lambda_i t} & te^{\lambda_i t} & \frac{1}{2}t^2e^{\lambda_i t} & \dots & \frac{1}{(r_i-1)!}t^{r_i-1}e^{\lambda_i t} \\ 0 & e^{\lambda_i t} & te^{\lambda_i t} & \dots & \frac{1}{(r_i-2)!}t^{r_i-2}e^{\lambda_i t} \\ \vdots & \vdots & \vdots & \ddots & \vdots \\ 0 & 0 & 0 & \dots & e^{\lambda_i t} \end{pmatrix}.$$

The general solution of equation (4) is given by the columns of $Y(t)$ which are

$$y(t) = \begin{pmatrix} 0 \\ \vdots \\ 0 \\ \frac{t^{r_i-1}}{(r_i-1)!}e^{\lambda_i t} \\ \frac{t^{r_i-2}}{(r_i-2)!}e^{\lambda_i t} \\ \vdots \\ e^{\lambda_i t} \\ 0 \\ \vdots \\ 0 \end{pmatrix}.$$

Having found such a general solution it is easy to transform it into a general solution of (2) by

$$x(t) = Cy(t). \tag{5}$$

Frequently one does not need the whole solution of a dynamical system but rather its asymptotic behaviour which can be seen easily by substituting the values of λ_i in the solution above.

2.1.2 Phase plane diagrams of two dimensional autonomous and linear systems near fixed points

Detailed explanations concerning this section can be found e.g. in [1] chapter III, 13.)

In this section we consider dynamical systems of the form (2) with $A \in \mathbb{R}^{2\times 2}$. Such systems allow to create phase plane diagrams which show trajectories of a dynamical system in the same phase plane. Each curve or point is related to a set of initial conditions.

Definition 2.1 *Given a dynamical system in* $\mathbb{R}^2$*,* $\phi : \mathbb{R} \times \mathbb{R}^2 \to \mathbb{R}^2$ *is called* flow $\phi_t(x)$ *of the dynamical system if the orbit is given by* $x(t) = \phi_t(x(0))$ *and*

- $\phi_0(x) = x$ *and*
- $\phi_t \circ \phi_s = \phi_t(\phi_s(x)) = \phi_{t+s}\ \forall t, s \in \mathbb{R}$

hold.

Definition 2.2 *If there is a point* $x_0 \in \mathbb{R}^2$ *with* $Ax_0 = 0$ *it is called* equilibrium point *or critical point.*

Such an equilibrium point is a *fixed point* of the flow of the dynamical system.

There is a classification of different types of equilibrium points which are distinguished by examining the eigenvalues of the dynamical system.

- If the system has two complex conjugated eigenvalues the trajectories surround the only fixed point. We distinguish three different types of this surrounding.
  - If $Re(\lambda) > 0$ the distance to the equilibrium point increases with time and the phase portrait is a *spiral source* which is plotted in figure 1a.
  - If $Re(\lambda) < 0$ the distance to the equilibrium point decreases with time and the phase portrait is a *spiral sink* which is plotted in figure 1b.
  - If $Re(\lambda) = 0$ the distance to the equilibrium point stays constant and the phase portrait is a *centre* plotted in figure 1c.
- If the eigenvalues of A are real, not zero and $\lambda_1 \neq \lambda_2$.
  - If $\lambda_1 > 0$ and $\lambda_2 > 0$ the phase portrait is a *nodal source* plotted in figure 2a.
  - If $\lambda_1 < 0$ and $\lambda_2 < 0$ the phase portrait is a *nodal sink* plotted in figure 2b.
  - If $\lambda_1 > 0$ and $\lambda_2 < 0$ (or vice versa) the phase portrait is a *saddle point* plotted in 2c.

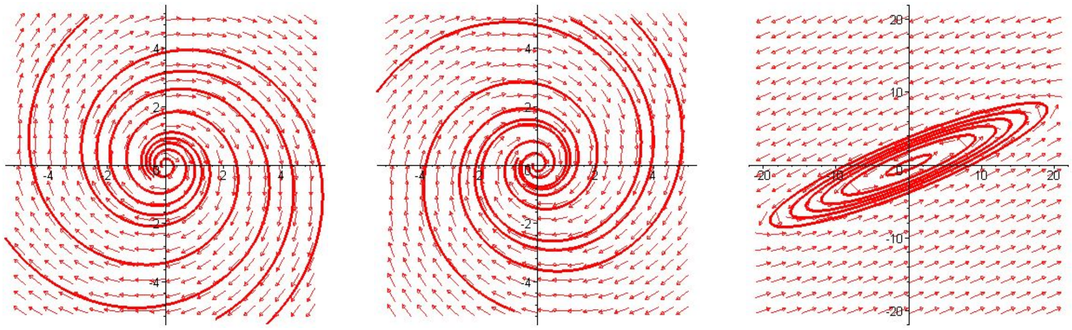

(a) Spiral source (b) Spiral sink (c) Centre

Figure 1: Phase portraits of a system with two complex eigenvalues

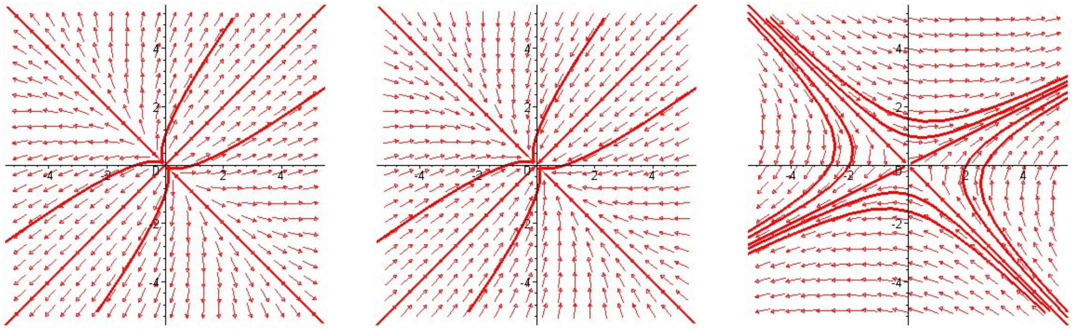

(a) Nodal source (b) Nodal sink (c) Saddle

Figure 2: Phase portraits of not equal and not zero real eigenvalues

- The next item is if $\lambda_1 = \lambda_2$ which is a special case of the above nodes. If there are two linearly independent eigenvectors of $\lambda_1 = \lambda_2$ the phase portrait is a star as shown in figure 3a and 3b. On the other hand if there is just one linearly independent eigenvalue the phase portrait is a node as in figure 3c.

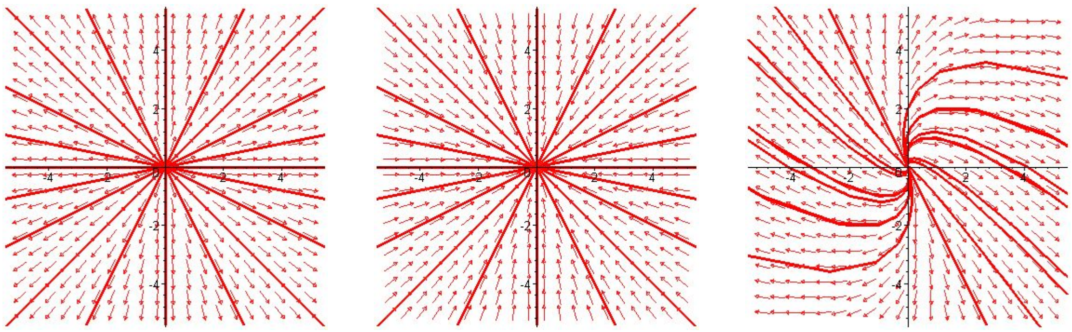

(a) Star source (b) Star sink (c) Degenerate star

Figure 3: Phase portraits if the two eigenvalues are equal and not zero

- The last special case is if one (or both) eigenvalues are zero. In this case the phase portrait looks like shown in the figure 4a and 4b.

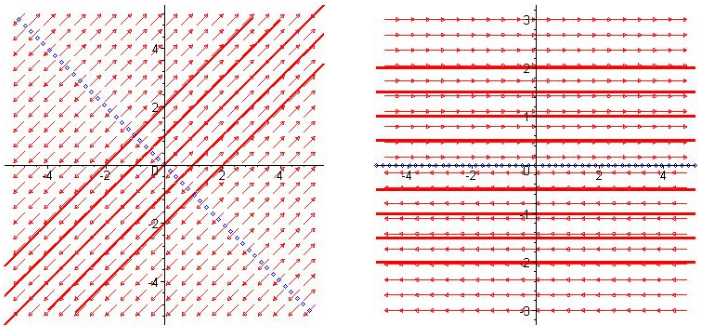

(a) $\lambda_1 = 0$, $\lambda_2 \neq 0$ (b) $\lambda_1 = \lambda_2 = 0$

Figure 4: Phase portrait if one or both eigenvalues are zero

2.1.3 Nonlinear systems and their linearisation

In the last sections we examined linear systems. Regrettably, examples of dynamical systems of physical use are in general nonlinear. Thus the next to deal with is linearisation. If a nonlinear system of differential equation is given, it is very useful to linearise it because one gets a lot of information of the system by analysing its linearisation. Now we examine systems like (1) with a nonlinear f.

Definition 2.3 *Consider x_0 as an equilibrium point of (1) then we call the system*

$$\dot{x} = Df(x_0)(x - x_0) \tag{6}$$

the linearisation *of (1) at x_0.*

There is a certain correlation between the orbits of (1) and those of (6). These correlations are summed up in the following theorem (see e.g. [30] p.315 or [25] p.114):

Theorem 2.4 Hartmann-Grobman
Suppose $f \in C^1(N)$ with N a neighbourhood of the equilibrium point x_0 and $A = Df(x_0)$ has no eigenvalue with $Re(\lambda) = 0$. Then there are two neighbourhoods E and F of the equilibrium point x_0 as well as a homoeomorphism $g : E \to F$ which transforms (with conservation of the direction) all trajectories of (6) belonging to E into trajectories of (1) belonging to F.

In other words:

Theorem 2.5 Hartmann-Grobman
Assume that $f \in C^\infty$ and that $Df(x_0)$ is invertible.

1. *If the linearised system (6) has a focus at the point x_0, then so does the nonlinear system (1).*
   (The same holds for saddle point, node, source or sink.)

2. *If the linearised system (6) has a centre at the point x_0, then the nonlinear system (1) has a centre or a focus.*

If the functional matrix is not invertible, such simple correspondences cannot be found.

2.2 Stability of Differential Equations

In this section we are going to examine the stability of the solution of a dynamical system. There are different terms of stability which will be introduced in the following. (What follows can be found in [30] p.306 ff and [1] p.219 ff.)

Definition 2.6 *Consider $\bar{x}(t)$ to be a solution of the system (1) for $t \in [a, \infty)$. The solution $\bar{x}(t)$ is said to be* stable (in the sense of Lyapunov) *if for every $t_0 \in [a, \infty)$ and $\epsilon > 0$ there exists $\delta(\epsilon, t_0) > 0$ such that for all other solutions $\tilde{x}(t)$ which are defined in $[a, \infty)$ hold:*

$$|\tilde{x}(t_0) - \bar{x}(t_0)| < \delta(\epsilon, t_0) \quad \Rightarrow \quad |\tilde{x}(t) - \bar{x}(t)| < \epsilon \quad \forall t \in [t_0 \infty)$$

(*analogous for the interval* $(-\infty, a]$).

If δ does not depend on t_0 we call the solution *uniformly stable.* We call a solution of a differential equation *unstable* if it is not stable.

Definition 2.7 *A solution $\bar{x}(t)$ is called* attractive *if there exists an $\alpha \in \mathbb{R}^+$ such that for every solution $\tilde{x}(t)$ for which*

$$|\tilde{x}(t_0) - \bar{x}(t_0)| < \alpha$$

holds, follows

$$\lim_{t \to \infty} |\tilde{x}(t) - \bar{x}(t)| = 0.$$

Definition 2.8 *A solution $\bar{x}(t)$ to the system (1) is called* asymptotically stable *if it is stable and attractive.*

2.2.1 Examples of different types of stability

The different types of phase plane diagrams tell about the stability behaviour. (This can be found e.g. in [30] p.188.)

- A centre is stable, but not asymptotically stable.
- A sink is asymptotically stable.
- A source is unstable.
- A saddle point is unstable.

3 Introduction to the physical problem

Up to now we have just examined several mathematical tools. Now we are going to introduce the physical problem.

General relativity is a theory of gravitation published by Albert Einstein in 1916 [8]. It describes gravity as a geometric property of space and time. The curvature of spacetime depends on the presence of matter and radiation. In the words of John Wheeler: "Spacetime tells matter how to move; matter tells spacetime how to curve."

The *Einstein equations* give the relation between the curvature of spacetime and the energy momentum tensor.

$$R_{\mu\nu} - \tfrac{1}{2} g_{\mu\nu} R = T_{\mu\nu} \tag{7}$$

In these equations $R_{\mu\nu}$ is the Ricci tensor, $g_{\mu\nu}$ the metric, R is the curvature scalar of the spacetime and $T_{\mu\nu}$ is the energy momentum tensor. These terms will be discussed in detail later on.

Spacetime is a *four-dimensional Lorentzian manifold* which is a four-dimensional manifold that appears locally like $\mathbb{R}^4$. (For detailed definition and discussion about manifolds see mathematical literature e.g. [31]). Such a manifold has a *metric* $g_{\mu\nu}$ of signature (- + + +). (Sometimes the signature (+ - - -) is also used in literature.)

In the Einstein equations (7) there is no distinction between space and time. Often it turns out to be useful to have a separation between space and time which can be achieved by the *3+1 formalism* (a separation into a three dimensional space and time) which gives a metric of the following form

$$ds^2 = g_{\mu\nu} dx^\mu dx^\nu = dt^2 + g_{ij} dx^i dx^j, \tag{8}$$

where t is the time coordinate and x^i (with i=1,2,3) are the spatial coordinates.

The metric is also called *first fundamental form* or *intrinsic curvature*. On the other hand the *second fundamental form*, also called *extrinsic curvature*, gives us the rate of change of the unit normal vector along a hypersurface (i.e. a submanifold of M of dimension $n-1$). It gives us information on how "the hypersurface deforms as it is carried forward along a normal." ([2] p.34)

Moreover we will need the concepts of *Bianchi models* which refer to a *spatially homogeneous* spacetime (i.e. the space part of the spacetime is homogeneous). The most important one in this work will be the one known as *Bianchi type I model* which is a generalisation of the FLRW model (see section 4.3). Bianchi models are multifunctional and up to date the most successful ones when trying to understand singularities in spacetime. Discussing all the different types of Bianchi models is beyond the scope of this work. Therefore we will just focus on the locally rotationally symmetric (LRS) Bianchi type I model which we will need later on. There are three diverse representations of LRS. Since all of these are fundamentally equal we consider through out this work the LRS model with $g_{22} = g_{33}$.

The line element of such a LRS Bianchi type I spacetime is

$$g_{\mu\nu}dx^\mu dx^\nu = -dt^2 + A^2(t)dx^2 + B^2(t)(dy^2 + dz^2) \tag{9}$$

with $t \in \mathbb{R}$ and $(x, y, z) \in \mathbb{R}^3$ or $(x, y, z) \in T^3$ which represents the three dimensional torus. Hence the metric is given by

$$g_{tt} = -1 \qquad g_{xx} = A^2 \qquad g_{yy} = g_{zz} = B^2 \qquad g_{ij} = 0 \ \ \forall i \neq j.$$

Moreover we need the *Christoffel symbols* which are given by

$$\Gamma^\alpha_{\beta\gamma} = \frac{1}{2}g^{\alpha\rho}(g_{\rho\beta,\gamma} + g_{\rho\gamma,\beta} - g_{\beta\gamma,\rho}) \tag{10}$$

where $g_{\rho\beta,\gamma}$ denotes differentiation of $g_{\rho\beta}$ with respect to x^γ.
The only Christoffel symbols that are not equal to zero in Bianchi type I are the following

$$\begin{aligned} \Gamma^t_{xx} &= A\dot{A} & \Gamma^t_{yy} &= \Gamma^t_{zz} = B\dot{B} \\ \Gamma^x_{xt} = \Gamma^x_{tx} &= \frac{\dot{A}}{A} & \Gamma^y_{yt} &= \Gamma^y_{ty} = \Gamma^z_{zt} = \Gamma^z_{tz} = \frac{\dot{B}}{B}. \end{aligned}$$

Now, because it will prove to be useful, we introduce new variables

$$k_1 = -\frac{\dot{A}}{A} \tag{11}$$

$$k_2 = -\frac{\dot{B}}{B}. \tag{12}$$

These two variables are the elements $k_1 = k^x_x$ and $k_2 = k^y_y = k^z_z$ belonging to the second fundamental form $k_{\mu\nu}(t)$ of the spatially homogeneous hypersurface $t = constant$ which are gained by

$$k^x_x = g^{x\alpha}k_{\alpha x} \tag{13}$$

$$k^y_y = g^{y\alpha}k_{\alpha y}. \tag{14}$$

The second fundamental form is symmetric, purely spatial and satisfies the equation

$$\partial_t g_{\mu\nu} = -2k_{\mu\nu}. \tag{15}$$

Using the two new variables the nonzero Christoffel symbols read

$$\begin{aligned} \Gamma^t_{xx} &= -A^2k_1 & \Gamma^t_{yy} &= \Gamma^t_{zz} = -B^2k_2 \\ \Gamma^x_{xt} = \Gamma^x_{tx} &= -k_1 & \Gamma^y_{yt} &= \Gamma^y_{ty} = \Gamma^z_{zt} = \Gamma^z_{tz} = -k_2. \end{aligned}$$

The *Riemann curvature tensor* is given by

$$R^\rho_{\sigma\mu\nu} = \partial_\mu\Gamma^\rho_{\nu\sigma} - \partial_\nu\Gamma^\rho_{\mu\sigma} + \Gamma^\rho_{\mu\lambda}\Gamma^\lambda_{\nu\sigma} - \Gamma^\rho_{\nu\lambda}\Gamma^\lambda_{\mu\sigma}. \tag{16}$$

This tensor can be used to create the *Ricci tensor*

$$R_{\alpha\beta} = R^{\rho}_{\alpha\rho\beta}. \tag{17}$$

The nonzero elements of the Ricci tensor are

$$\begin{aligned} R_{tt} &= \dot{k}_1 - k_1^2 + 2\dot{k}_2 - 2k_2^2 \\ R_{xx} &= A^2 k_1(k_1 + 2k_2) - A^2 \dot{k}_1 \\ R_{yy} &= R_{zz} = B^2 k_2(k_1 + 2k_2) - B^2 \dot{k}_2. \end{aligned}$$

Furthermore the *curvature scalar* can be derived from the Riemann curvature tensor and is given by

$$R = g^{\alpha\beta} R_{\alpha\beta} = R^{\alpha}_{\alpha}. \tag{18}$$

Using the nonzero elements of the Ricci tensor the curvature scalar is given by

$$R = -2\dot{k}_1 + 2k_1^2 - 4\dot{k}_2 + 6k_2^2 + 4k_1 k_2.$$

These results are needed for the *Einstein equations* which are (see (7)),

$$R_{\mu\nu} - \tfrac{1}{2} g_{\mu\nu} R = T_{\mu\nu}, \tag{19}$$

where $T_{\mu\nu}$ is the energy momentum tensor which will be specified later on.

4 LRS Bianchi type I with perfect fluids source

The aim of this section is to solve the Einstein equations for a LRS Bianchi type I model with a perfect fluid source. First we will establish the general setup and then we will discuss in detail possible solutions of the Einstein equations. The first is to specify the energy momentum tensor.

4.1 Energy momentum tensor of a perfect fluid

Perfect Fluids are fluids that satisfy the Euler equation

$$\nabla_\mu T^{\mu\nu} = 0.$$

Indicating the energy density ρ, the pressure p and the 4-velocity u^μ the energy momentum tensor looks like

$$\begin{aligned} T_{\mu\nu} &= \rho u_\mu u_\nu + p(g_{\mu\nu} + u_\mu u_\nu) \\ &= (\rho + p)u_\mu u_\nu + p g_{\nu\mu} \end{aligned}$$

and thus

$$T^\mu_{\ \nu} = diag(-\rho, p, p, p).$$

We suppose that the two variables ρ and p satisfy a linear relation

$$p = w\rho \tag{20}$$

with a constant $w \in (-1/3, 1)$. Different w describe different equations of state. For example $w = 0$ gives the equation for dust and $w = 1/3$ represents the one for radiation. The thermodynamic character is described by a state equation of ρ.

4.2 Einstein equations for LRS Bianchi type I with a perfect fluid source

Now using everything we gained so far we can examine closer the Einstein equations (7). The only nonzero terms are the following

$$\begin{aligned} 2\dot{k_2} - 3k_2^2 &= p \\ \dot{k_1} - k_1^2 + \dot{k_2} - k_2^2 - k_1 k_2 &= p \\ k_2^2 + 2k_1 k_2 &= \rho. \end{aligned}$$

Reformulating these equations we get

$$\dot{k_1} = k_1^2 + 2k_1 k_2 + \frac{1}{2}(p - \rho) \tag{21}$$

$$\dot{k_2} = k_1 k_2 + 2k_2^2 + \frac{1}{2}(p - \rho) \tag{22}$$

$$k_2^2 + 2k_1 k_2 = \rho \tag{23}$$

and from equation (11) and (12) we get

$$\begin{aligned} \dot{A} &= -k_1 A && (24)\\ \dot{B} &= -k_2 B. && (25) \end{aligned}$$

What we have found are two evolution equations (differential equations) see (21) and (22) and one constraint equation (algebraic equation) see (23). Now we will examine some initial value problems of these equations.

4.3 Friedmann-Lemaître-Robertson-Walker (FLRW) metric

The first metric we will examine is the so called Friedmann-Lemaître-Robertson-Walker metric (or just Friedmann metric). The assumptions for this model are homogeneity and isotropy (called *Cosmological Principle*). If we take into account these assumptions we gain

$$k_1 = k_2$$

for a certain time t. Comparing the right hand sides of the two equations (21) and (22) one can easily see that they are equal if $k_1 = k_2$ from which we can conclude that $\dot{k}_1 = \dot{k}_2$ and thus $k_1 = k_2$ for all times. This implies (see equations (24) and (25)) that $A = B$ for all times. Thus the metric is of the form

$$-dt^2 + A^2(t)(dx^2 + dy^2 + dz^2) \qquad (26)$$

where $A(t)$ is called *scale factor*.

The next step is to search for the behaviour of $A(t)$. Setting $k_1 = k_2$ in the Einstein equations (21)-(23) and using equation (20) we get

$$\begin{aligned} \dot{k}_1 &= 3k_1^2 + \tfrac{1}{2}(w-1)\rho && (27)\\ \rho &= 3k_1^2. && (28) \end{aligned}$$

Equation (28) can be used to substitute ρ in equation (27). We gain a differential equation with one variable which can integrate easily and gives the result

$$k_1 = -\frac{2}{3(1+w)t}.$$

The constant of integration is set to zero. This can be done because the constant of integration is just a translation of time which does not have any effect on our calculations.

Our aim is to get the time dependence of the metric. We use equation (11) and get

$$g_{xx} = g_{yy} = g_{zz} = A(t)^2 = at^{\frac{4}{3(1+w)}}$$

with a constant of integration $\sqrt{a}$. The constant a could be set equal to 1 because we could absorb it by rescaling dt, dx, dy and dz. Such a rescaling would not have any effect on our discussions. Nevertheless we will keep it to get a more general result.

Our considerations give the following metric

$$-dt^2 + at^{\frac{4}{3(1+w)}}(dx^2 + dy^2 + dz^2).$$

In section 6.3 we will discuss whether the assumptions of this section are applicable and whether they fit to the observation data or not.

4.4 Kasner metric

Now we will discuss the so called Kasner metric which is a solution of the Einstein equations for vacuum. The vacuum gives $p = \rho = 0$.
Substituting this in the equation system (21)-(23) we get

$$\begin{aligned} \dot{k}_1 &= k_1^2 + 2k_1k_2 & (29) \\ \dot{k}_2 &= k_1k_2 + 2k_2^2 & (30) \\ k_2^2 + 2k_1k_2 &= 0. & (31) \end{aligned}$$

One solution of these equations is obvious since equation (31) holds if

$$k_2 = 0.$$

Using this and equation (12) we find

$$B = \sqrt{b}.$$

Once found, we can substitute $k_2 = 0$ in equation (29) and get

$$\dot{k}_1 = k_1^2.$$

This is a differential equation with just one variable and can be solved by integration which gives

$$k_1 = -\frac{1}{t}.$$

The constant of integration is set to zero for the same reason as in the previous section. Using this and equation (11) we find

$$A = \sqrt{a}t \tag{32}$$

with a constant $\sqrt{a}$. Hence the first solution called *Taub solution* is given by

$$-dt^2 + at^2dx^2 + bdy^2 + bdz^2$$

with two constants a and b. These constants could be absorbed by rescaling dt, dx, dy and dz but we keep it for a more general metric.

Moreover there is a second Kasner solution. To get the second solution we can use equation (31) to decouple equation (30) and get

$$\dot{k}_2 = \frac{3}{2}k_2^2$$

which can be solved for k_2. A straightforward calculation gives

$$k_2 = -\frac{2}{3t}.$$

Integrating (using equation (12)) and setting the constant of integration equal to $\sqrt{b}$ gives

$$B = \sqrt{b}t^{\frac{2}{3}}.$$

Hence the first metric coefficient is found. We can use these results to calculate the second metric coefficient, via

$$k_1 = \frac{1}{3t}.$$

Equation (24) leads to

$$A = \sqrt{a}t^{-\frac{1}{3}}$$

with a constant of integration $\sqrt{a}$.
Thus the second Kasner solution called *non-flat Kasner solution* is given by the metric

$$-dt^2 + at^{-\frac{2}{3}}dx^2 + bt^{\frac{4}{3}}(dy^2 + dz^2) \tag{33}$$

with two constants a and b.

The results and assumptions of this section are also discussed later. See section 6.4 for further information how this model fits to the observed data.

5 LRS Bianchi type I with anisotropic matter

The set-up is the same as in the example above but instead of perfect fluids anisotropic matter will be used. The Einstein equations have to be reformulated to be solved. We will use the same reformulation as in [4].

5.1 Anisotropic matter models

In the last section we used perfect fluid models. Now we search for more general solutions of the Einstein equations. The anisotropic matter model used generalises naturally a model with a perfect fluid source. To find a solutions the Einstein equations some information about the energy momentum tensor is needed. We will not use a specific energy momentum tensor but rather use constraints to get a certain class of energy momentum tensors. Examples which satisfy our anisotropic models are: collisionless matter (Vlasov matter) and elastic materials (for detailed information see [4, section 3]).

Since the pressure in this model is not isotropic we need the *principal pressures* p_i. These principal pressures are entries of the energy momentum tensor as

$$\begin{aligned} p_1 &= T^1{}_1 \\ p_2 &= T^2{}_2 \\ p_3 &= T^3{}_3. \end{aligned}$$

If $p_1 = p_2 = p_3$ we have the energy momentum tensor of a perfect fluid.

As we compare the anisotropic model to the isotropic one we define the *isotropic pressure*

$$p = \tfrac{1}{3}(p_1 + p_2 + p_3).$$

We also call p isotropic pressure because if $p_1 = p_2 = p_3$, p turns out to be the isotropic pressure of the perfect fluid model.

Furthermore we need the *rescaled principal pressures* w_i which are given by

$$w_i = \frac{p_i}{\rho} \tag{34}$$

w is defined via

$$w = \tfrac{1}{3}(w_1 + w_2 + w_3).$$

If we assume $p_1 = p_2 = p_3$ the new variable w turns out to be the same w as we used in the perfect fluid model.

In addition we suppose there is a linear relation between the isotropic pressure p and the density ρ through the relation

$$p = w\rho \tag{35}$$

with $w \in (-1/3, 1)$.

The next step is to introduce new variables s and s_i (i=x,y,z)

$$\begin{aligned} s &= \frac{g^{yy}}{g^{xx}+g^{yy}+g^{zz}} \\ &= \frac{A^2}{B^2+2A^2} \end{aligned} \tag{36}$$

$$s_i = \frac{g^{ii}}{g^{xx}+g^{yy}+g^{zz}}. \tag{37}$$

These variables live in the interior of

$$\chi = \{0 < s_i < 1 : s_x + s_y + s_z = 1\}.$$

Moreover we need an anisotropy function $u(s)$ defined as

$$w_2(1-2s, s, s) = w_3(1-2s, s, s) = u(s) \tag{38}$$

and as a consequence

$$w_1(1-2s, s, s) = 3w - 2u(s).$$

The next to introduce is the anisotropy parameter β.

$$\beta = 2\frac{w-u(0)}{1-w} = 4\frac{u(\frac{1}{2})-w}{1-w} \tag{39}$$

This newly introduced parameter gives us information on the size of the deviation of the anisotropic matter model and the isotropic one. If $\beta = 0$ this refers to a perfect fluid matter model near a singularity.

After all these definitions which can be seen above we are now ready to start our calculations.

5.2 Einstein equation for LRS Bianchi type I with anisotropic matter sources

In the previous section we introduced a specific class of energy momentum tensors, those for anisotropic matter. This energy momentum tensor can be inserted into the Einstein equations (7). In analogy to the equations (21) – (23) we find a system of equations with anisotropic matter

$$\dot{k}_1 = k_1^2 + 2k_1k_2 - p_1 + \frac{1}{2}(p_1 + 2p_2 - \rho) \tag{40}$$

$$\dot{k}_2 = k_1k_2 + 2k_2^2 - p_2 + \frac{1}{2}(p_1 + 2p_2 - \rho) \tag{41}$$

$$k_2^2 + 2k_1k_2 = \rho. \tag{42}$$

Once more the first two equations (40) and (41) are evolution equations and the last one (42) is a constraint equation.

It is useful to define a new variable which is the traceless extrinsic curvature (see section 3) taken with a negative sign

$$\sigma^\mu_\nu = -(k^\mu_\nu - \frac{1}{3}\mathrm{tr}(k)\delta^\mu_\nu). \tag{43}$$

In addition we define the variables σ_+ and H as

$$\begin{aligned} H &= -\tfrac{1}{3}(k_1 + 2k_2) && (44)\\ \sigma_+ &= \sigma^y_y = \tfrac{1}{3}k_1 - \tfrac{1}{3}k_2 && (45)\end{aligned}$$

where H is the *Hubble parameter* (see section 6.3 for more information) and σ_+ is the shear variable.

The equations (40) − (42), which we have gained from Einstein equations and taken into account the anisotropic matter model of section 5.1, are very complicated. Thus we simplify them by reformulating them with new variables. The new variables H and σ_+ allow us to write k_1 and k_2, through transformation of equation (44) and (45), as

$$\begin{aligned} k_1 &= -H + 2\sigma_+ && (46)\\ k_2 &= -H - \sigma_+. && (47)\end{aligned}$$

The constraint (42) can be reformulated using the new variables, which gives

$$H^2 = \tfrac{\rho}{3} + \sigma_+^2. \tag{48}$$

Now we have got a new constraint equation. Hence the next logical step is to search for evolution equations for the new variables. To find such an equation we differentiate the equation for s (36). Then employing equation (11) and (12) as well as the definition of σ_+ of equation (45) we get

$$\begin{aligned} \dot{s} &= \frac{2A\dot{A}(B^2 + 2A^2) - (2B\dot{B} + 4A\dot{A})A^2}{(B^2 + A^2)^2} && (49)\\ &= -6s(1 - 2s)\sigma_+. \end{aligned}$$

In analogy to this we find an evolution equation for σ_+ by integrating (45), using the equations (40) − (42) as well as the definitions of H and w_i given by (44) and (34).

$$\begin{aligned} \dot{\sigma}_+ &= \tfrac{1}{3}\dot{k}_1 - \tfrac{1}{3}\dot{k}_2 && (50)\\ &= -3H\sigma_+ + (w_2 - w)\rho \end{aligned}$$

Additionally we need the derivation of H. We derive the definition of H given by equation (44) and use the system (40)−(42), (48) as well as (34)−(35) to reformulate the equation.

$$\begin{aligned} \dot{H} &= -\frac{1}{3}\dot{k}_1 - \frac{2}{3}\dot{k}_2 && (51)\\ &= -H^2 - 2\sigma_+^2 - \frac{1}{6}(1 + 3w)\rho \end{aligned}$$

The next to define is

$$\Sigma_+ = \sigma_+/H. \tag{52}$$

Moreover we transform $\frac{\partial}{\partial t}$, represented by a dot, to $\frac{\partial}{\partial \tau}$, represented by a prime, by

$$\frac{\partial}{\partial \tau} = \frac{1}{H}\frac{\partial}{\partial t} \tag{53}$$

which is called *Hubble normalisation*. Employing these transformations as well as equations (51) and (38) we get out of (49) and (50) the dynamical system

$$\begin{aligned} \Sigma_+' &= -3(1-\Sigma_+^2)(\tfrac{1}{2}(1-w)\Sigma_+ - (u(s)-w)) && (54)\\ s' &= -6s(1-2s)\Sigma_+. && (55) \end{aligned}$$

Since now we have got the evolution equations of the new variables Σ_+ and s we need a belonging constraint equation, for which we define the normalized energy density

$$\Omega = \tfrac{\rho}{3H^2}. \tag{56}$$

This gives a constraint equation (see (48))

$$\Sigma_+^2 + \Omega = 1. \tag{57}$$

As the energy density $\rho \geq 0$ the normalised energy density $\Omega \geq 0$. Hence the constraint (57) leads to $\Sigma_+ \in (-1, 1)$ and because of $0 < s < \frac{1}{2}$ the system (54) and (55) is defined on the state space

$$S = \{(\Sigma_+, s) \in (-1, 1) \times (0, \tfrac{1}{2})\}. \tag{58}$$

Moreover the system can be extended to the boundary of the state space in a regular way.

Appendix A contains phase portraits (see section 2.1.2) of the system (54) and (55) for different values of w and β. We used linear approximation for $u(s)$ to create the portraits. As one can see the phase portraits depend on the two values w and β. In these phase portraits there are different equilibrium points which will be needed later on to find a solution of the dynamical system (54) and (55).

In the following we need the transformed Hubble parameter which we get by using equation (51), (52), (56) and (57)

$$\begin{aligned} H' &= \frac{1}{H}\dot{H} \\ &= -\frac{3}{2}H\left(1 + w + \Sigma_+^2(1-w)\right). && (59) \end{aligned}$$

5.3 Equilibrium points

Since we search for solutions of the system (54) and (55) we will examine the solutions at the equilibrium points and later on we will linearise the system near the only fix point in the interior of the state space (58). The linearisation also tells us how the real solution behaves near the equilibrium point (see section 2.1.3).

The equilibrium points on the boundary which always exist are

$$T_b : (\Sigma_+, s) = (-1, 0) \qquad Q_b : (\Sigma_+, s) = (1, 0)$$
$$T_a : (\Sigma_+, s) = (-1, \tfrac{1}{2}) \qquad Q_a : (\Sigma_+, s) = (1, \tfrac{1}{2}).$$

5.3.1 Taub points

The two points T_b and T_a are called *Taub points* because they refer to the Taub solution which is represented by the spatial metric

$$g_{xx} = at^2 \qquad g_{yy} = g_{zz} = b \tag{60}$$

with positive constants a and b (see section 4.4). This can be seen very easily. We substitute the rescaled variable Σ_+ ($\Sigma_+ = -1$ for both Taub points) in equation (52) which gives

$$\sigma_+ = -H.$$

Employing this and equation (47) we see that

$$k_2 = 0$$

which leads via equation (12) to $\dot{B} = 0$. Integration of $\dot{B}$ gives

$$B = \sqrt{b}$$

with a constant of integration $\sqrt{b}$ and thus

$$g_{yy} = g_{zz} = b.$$

The next step is to search for the behaviour of g_{xx}. The condition $\Sigma_+ = -1$ used in equation (57) gives $\Omega = 0$. Because of this we know that the matter model has to be a vacuum model. Now the rescaled variable H' (equation (59)) is

$$H' = -3H. \tag{61}$$

Solving that for H gives

$$H = \text{const } e^{-3\tau}. \tag{62}$$

This equation tells us about the τ dependence of H. As we search for H depending on t, not τ, we have to find a retransformation which can be achieved by putting the found H into the Hubble normalisation (53) i.e.

$$dt = \frac{1}{\text{const}} e^{3\tau} d\tau.$$

If we integrate this equation the constant of integration can be set equal to zero since a constant of integration in this equation is just a translation of time and does not have any effect on our results. Moreover we eliminate the other constant const by setting it equal to one which does not have any effect on our calculations either. Thus the retransformation is

$$\tau = \frac{1}{3}\ln(3t).$$

Using this retransformation we finally get H depending on t

$$H = \frac{1}{3t}. \tag{63}$$

Since we found $k_2 = 0$ equation (44) reads

$$H = -\frac{1}{3}k_1$$

and equation (11) gives

$$H = \frac{\dot{A}}{3A}.$$

Employing the results for H from above we find

$$A = \sqrt{a}t$$

with a positive constant $\sqrt{a}$. Hence

$$g_{xx} = a\ t^2.$$

Thus we have found the spatial metric referring to the Taub solution. This metric will be examined closer in section 6.4.

5.3.2 Non-flat LRS points

The two equilibrium points Q_b and Q_a are called *non-flat LRS points* as they refer to the non-flat LRS solution represented by the spatial metric

$$g_{xx} = at^{-2/3} \qquad g_{yy} = g_{zz} = bt^{4/3} \tag{64}$$

with two positive constants a and b (see section 4.4). Analogous to the previous section 5.3.1 one can easily see that Q_b and Q_a are non-flat LRS solutions which are also vacuum solutions. Calculations carried out in a similar way to the former section give also (see (63))

$$H = \frac{1}{3t}.$$

The equation for σ_+ is different, namely

$$\sigma_+ \ = \ H$$

which in turn gives a different k_2

$$k_2 \;=\; -2H.$$

Using that in equation (12) we find

$$\frac{\dot{B}}{B} \;=\; \frac{2}{3t}$$

which can be integrated to

$$B = \sqrt{b}t^{2/3}$$

with a constant $\sqrt{b}$. Hence

$$g_{yy} = g_{zz} = b\ t^{4/3}.$$

Employing equation (44) leads to

$$A = \sqrt{a}t^{-1/3}$$

which gives us the metric element

$$g_{xx} = a\ t^{-2/3}.$$

Now we have found the metric corresponding to the non-flat LRS Kasner solution. For further discussion about this metric see section 6.4.

5.3.3 Equilibrium points depending on the anisotropy parameter

There are two more equilibrium points which refer to non vacuum solutions. These fixed points depend on the anisotropy parameter β

$$\begin{aligned} R_b : (\Sigma_+, s) \;&=\; (-\beta, 0) \quad \text{which exists if} \quad \beta \in (-1, 1) \\ R_a : (\Sigma_+, s) \;&=\; (\tfrac{\beta}{2}, \tfrac{1}{2}) \quad \text{which exists if} \quad \beta \in (-2, 2). \end{aligned}$$

We have got these limitations of β since Σ_+ is just defined on the interval $(-1, 1)$.

Firstly we start with R_b. If we examine (59) using this point we get

$$H' = -\tfrac{3}{2}H\,(1 + w + \beta^2(1-\omega))$$

which gives via straight forward calculation the Hubble parameter

$$H = \text{const}\ e^{-\frac{3}{2}\,(1 + w + \beta^2(1-\omega))\,\tau}$$

with an integration constant const. (This integration constant can be set equal to one since this does not have any effect on our calculations.) Employing the Hubble normalisation (53) we gain

$$\tau = \tfrac{2}{3(1+w+\beta^2(1-\omega))}\ln(\tfrac{3}{2}\,(1 + w + \beta^2(1-\omega))\,t)$$

and thus

$$H = \frac{2}{3\,(1 + w + \beta^2(1-\omega))\,t}. \tag{65}$$

Reformulating the equations (46) and (47) using equation (52) and the value for Σ_+ of R_b results in

$$\begin{aligned} k_1 &= -(1+2\beta)H && (66)\\ k_2 &= -(1-\beta)H. && (67) \end{aligned}$$

The first of these two equations (66) leads to (via equation (11))

$$\frac{\dot{A}}{A} = \frac{2+4\beta}{3\,(1 + w + \beta^2(1-\omega))\,t}$$

and the equation for k_2 (67) gives, employing (12),

$$\frac{\dot{B}}{B} = \frac{2-2\beta}{3\,(1 + w + \beta^2(1-\omega))\,t}.$$

The above two equations can be integrated which leads to

$$\begin{aligned} A &= \sqrt{a}\; t^{\frac{2+4\beta}{3(1+w+\beta^2(1-\omega))}}\\ B &= \sqrt{b}\; t^{\frac{2-2\beta}{3(1+w+\beta^2(1-\omega))}} \end{aligned}$$

with two constants of integration $\sqrt{a}$ and $\sqrt{b}$. Hence the metric has got the form

$$\begin{aligned} g_{xx} &= a\; t^{\frac{4+16\beta}{3(1+w+\beta^2(1-\omega))}}\\ g_{yy} &= g_{zz} = b\; t^{\frac{4-4\beta}{3(1+w+\beta^2(1-\omega))}}. \end{aligned} \tag{68}$$

In analogy to this we work out the behaviour at the point R_a which gives

$$H = \frac{2}{3\,(1 + w + \beta^2/4(1-\omega))\,t}. \tag{69}$$

and further to

$$\begin{aligned} k_1 &= -(1-\beta)H\\ k_2 &= -(1+\frac{\beta}{2})H. \end{aligned}$$

Thus the metric reads

$$\begin{aligned} g_{xx} &= a\; t^{\frac{4-4\beta}{3(1+w+\beta^2/4(1-\omega))}}\\ g_{yy} &= g_{zz} = b\; t^{\frac{4+2\beta}{3(1+w+\beta^2/4(1-\omega))}} \end{aligned} \tag{70}$$

with the two constants a and b.

These two metrics (68) and (70) depend both on the anisotropy parameter β. If $\beta = 0$ (which refers to isotropy) is inserted into these two metrics the result is the Friedmann metric of section 4.3 which describes an isotropic matter model. Observational relevance of these metrics is discussed in section 6.5.1.

5.3.4 Equilibrium point in the interior

There is just one equilibrium point in the interior of the state space S (58). This point is

$$F : (\Sigma_+, s) = (0, \bar{s}) \text{ with } \bar{s} \in (0, \tfrac{1}{2}) \text{ the unique solution of } u(\bar{s}) = w.$$

This fixed point refers to the isotropic fluid FLRW solution of section 4.3 which is

$$g_{xx} = g_{yy} = g_{zz} = at^{\frac{4}{3(1+w)}}.$$

To see this one just has to carry out a straight forward calculation. We start again with H' of equation (59). Hence

$$H' = -\frac{3}{2}H(1 + w)$$

which gives (omitting the constant of integration)

$$H = e^{-\frac{3}{2}(1 + w)\tau}.$$

Employing the Hubble normalisation (53) we get the transformation

$$\tau = \tfrac{2}{3(1+w)} \ln\left(\tfrac{3}{2}(1 + w)t\right) \tag{71}$$

and thus

$$H = \frac{2}{3(1 + w)t}. \tag{72}$$

The coordinate $\Sigma_+ = 0$ gives (see (46) and (47))

$$k_1 = -H \tag{73}$$

$$k_2 = -H \tag{74}$$

which lead to

$$k_1 = k_2. \tag{75}$$

Integration results in the Friedmann metric

$$g_{xx} = g_{yy} = g_{zz} = a\ t^{\frac{4}{3(1+w)}} \tag{76}$$

with a constant of integration $\sqrt{a}$. Later, in section 6.3, we will discuss the experimental relevance of this metric.

5.4 Linearisation around equilibrium point F

Up to now we have just examined points on the boundary of the state space (58) and one point in the interior of it. Now we linearise the dynamical system (54) and (55) near F to find out what the solution looks like in first order approximation around F. (Information about linearisation around an equilibrium point can be read up in section 2.1.3).

The linearisation around the equilibrium point F, given by $(\Sigma_+, s) = (0, \bar{s})$ with $\bar{s} \in (0, \frac{1}{2})$ the unique solution of $u(s) = w$, is

$$\begin{aligned} \Sigma_+' &= -\tfrac{3}{2}(1-w)\Sigma_+ + 3\tfrac{du}{ds}(\bar{s})(s-\bar{s}) \\ s' &= -6\bar{s}(1-2\bar{s})\Sigma_+. \end{aligned} \tag{77}$$

The eigenvalues and eigenvectors of this system are

$$\begin{aligned} \lambda_\pm &= -\tfrac{3}{4}\left(1 - w \mp \sqrt{(1-w)^2 - 32\bar{s}u'(\bar{s})(1-2\bar{s})}\right) \\ ev_\pm &= \left(\tfrac{4u'(\bar{s})}{1-w\pm\sqrt{(1-w)^2-32\bar{s}u'(\bar{s})(1-2\bar{s})}}, 1\right). \end{aligned}$$

From now on let

$$C = \sqrt{(1-w)^2 - 32\bar{s}u'(\bar{s})(1-2\bar{s})} \tag{78}$$

which leads to the following form of the eigenvalues and eigenvectors

$$\begin{aligned} \lambda_\pm &= -\tfrac{3}{4}(1 - w \mp C) \\ ev_\pm &= \left(\tfrac{4u'(\bar{s})}{1-w\pm C}, 1\right). \end{aligned}$$

Having now linearised the equations and gained the eigenvectors and eigenvalues we can examine the solutions of the linearised system which depend on u'.

- The first case is $u'(\bar{s}) < 0$.

  This implies $C > 0$ and $C > 1 - w$. Hence the eigenvalues satisfy $\lambda_+ > 0$, $\lambda_- < 0$ and $\lambda_+ > \lambda_-$ which lead to a phase portrait that looks like a saddle (see figure 2c). Such an equilibrium point is according to section 2.2 unstable. The Σ_+ reads

  $$\Sigma_+ = c_1\tfrac{4u'(\bar{s})}{1-w+C}\exp\left(\tfrac{3}{4}(1-w-C)\tau\right) + c_2\tfrac{4u'(\bar{s})}{1-w-C}\exp\left(-\tfrac{3}{4}(1-w+C)\tau\right). \tag{79}$$

- The next to look at is the case $u'(\bar{s}) = 0$.

  Now the phase portrait looks like figure 4a. As this can be seen as a special case of the following classification we will not treat it separately in the following.

- The third case is given by $u'(\bar{s}) > 0$ and $u'(\bar{s}) \leq \frac{(1-w)^2}{32\bar{s}(1-2\bar{s})}$.

  This leads to $C > 0$ and $C < 1 - w$. Here the eigenvalues satisfy $\lambda_+ < 0$, $\lambda_- < 0$ and $\lambda_+ > \lambda_-$ which give a phase portrait of a nodal sink as shown in figure 2b which is asymptotically stable (see section 2.2).
  Now Σ_+ reads

  $$\Sigma_+ = c_1\tfrac{4u'(\bar{s})}{1-w+C}\exp\left(-\tfrac{3}{4}(1-w-C)\tau\right) + c_2\tfrac{4u'(\bar{s})}{1-w-C}\exp\left(-\tfrac{3}{4}(1-w+C)\tau\right). \tag{80}$$

- The last case is $u'(\bar{s}) > \frac{(1-w)^2}{32\bar{s}(1-2\bar{s})}$.

  In this case both eigenvalues are complex and the real parts satisfy $Re(\lambda_\pm) < 0$ with a phase portrait of a spiral sink like in figure 1b which is also asymptotically stable as in the above case.
  This time Σ_+ reads, with the new variable $\tilde{C} = -iC$,

$$\Sigma_+ = \exp\left(-\tfrac{3}{4}(1-w)\tau\right)\left(\tfrac{4c_1 u'(\bar{s})(1-w)}{(1-w)^2+\tilde{C}^2}\cos(\tilde{C}\tau) - \tfrac{4c_2 u'(\bar{s})\tilde{C}}{(1-w)^2+\tilde{C}^2}\sin(\tilde{C}\tau)\right). \tag{81}$$

The case of F as a saddle is unstable and only tends to F in one characteristic direction. Thus it is insignificant. Nevertheless we start our considerations with this case because the calculations are the most simply ones but with the same ideas as in the other asymptotically stable cases.

5.4.1 F as a saddle ($u'(\bar{s}) < 0$)

Before starting our calculations we can simplify Σ_+. When the phase portrait is a saddle there is just one trajectory which tends to the equilibrium point F. That trajectory is the one according to the negative eigenvalue and the one we are interested in. Thus we write Σ_+ as

$$\Sigma_+ = c_2\tfrac{4u'(\bar{s})}{1-w-C}\exp\left(-\tfrac{3}{4}(1-w+C)\tau\right). \tag{82}$$

Now we have got a linear system and a solution of Σ_+ which allows us to search for g_{ab}. Making use of the equations (15) and (43) the metric coefficients are given by

$$\partial_t g_{ab} = 2g_{ac}(\sigma^c_b - \tfrac{1}{3}tr(k)\delta^c_b).$$

We will start with the calculation of g_{yy}. Firstly we transform the above equation using equation (44) and (45) as well as (52) which leads to

$$\begin{aligned}\partial_t g_{yy} &= 2g_{2c}(\sigma^c_2 - \tfrac{1}{3}tr(k)\delta^c_2)\\ &= 2g_{yy}(\sigma^2_2 - \tfrac{1}{3}tr(k)\delta^2_2)\\ &= 2g_{yy}H(\Sigma_+ + 1).\end{aligned}$$

The first step is valid because all g_{yc} with $c \neq y$ are zero (analogous for σ^c_y and δ^c_y). In the above equation the right hand side depends on τ and the left hand side depends on t. Thus we transform ∂_t to ∂_τ using the Hubble normalisation (53).

$$\begin{aligned}\partial_\tau g_{yy} &= \frac{\partial_t}{H}g_{yy}\\ &= 2g_{yy}(\Sigma_+ + 1)\end{aligned} \tag{83}$$

Employing Σ_+ of equation (82) and integrating the above equation give

$$\ln g_{yy} = -c_2\tfrac{32u'(\bar{s})}{3(1-w+C)(1-w-C)}\exp\left(-\tfrac{3}{4}(1-w+C)\tau\right) + 2\tau + \tilde{g_{yy}}$$

and thus

$$g_{yy} = \exp\left(-c_2\tfrac{32u'(\bar{s})}{3(1-w+C)(1-w-C)}\exp\left(-\tfrac{3}{4}(1-w+C)\tau\right) + 2\tau + \tilde{g_{yy}}\right).$$

Now we examine the metric in the future direction. Since the term $\exp\left(-\frac{3}{4}(1-w+C)\tau\right) \to 0$ for $\tau \to \infty$, g_{yy} can be simplified by using the Taylor approximation of the exponential function around zero. The second order Taylor approximation is given by

$$e^{\epsilon} = 1 + \epsilon + O(\epsilon^2) \quad \text{with small } \epsilon. \tag{84}$$

We will examine the first order approximation. Thus we eliminate quadratic terms (and terms of higher order). Employing this the coefficient g_{yy} with a constant $\tilde{\tilde{g_{yy}}} = \exp(\tilde{g_{yy}})$ reads

$$g_{yy} \;=\; \tilde{\tilde{g_{yy}}} e^{2\tau} \left(1 - c_2 \tfrac{32u'(\bar{s})}{3(1-w+C)(1-w-C)} \exp\left(-\tfrac{3}{4}(1-w+C)\tau\right)\right). \tag{85}$$

This equation tells us in which way g_{yy} depends on τ. Since we search for a dependency on t we need some relation between τ and t which can be found by integrating the Hubble normalisation (53).

The time-rescaled Hubble parameter is given by equation (59) which is a first order differential equation. Hence the solution (with Σ_+ of equation (82)) is

$$H = H_0 \exp\left(-\tfrac{3}{2}(1+w)\tau\right) \exp\left(-\tfrac{3}{2}(1-w)\int \Sigma_+^2 d\tau\right). \tag{86}$$

In order to compute this H we need $\int \Sigma_+^2 d\tau$.

$$\begin{aligned}\Sigma_+^2 &= c_2^2 \tfrac{16u'(\bar{s})^2}{(1-w-C)^2} \exp\left(-\tfrac{3}{2}(1-w+C)\tau\right)\\ \int \Sigma_+^2 d\tau &= -c_2^2 \tfrac{32u'(\bar{s})^2}{3(1-w-C)^2(1-w+C)} \exp\left(-\tfrac{3}{2}(1-w+C)\tau\right)\end{aligned}$$

We know Σ_+ behaves like $e^{-\tau}$ which means Σ_+^2 behaves like $e^{-2\tau}$ and moreover $\int \Sigma_+^2 d\tau \to 0$ if $\tau \to \infty$. Thus if $\tau \to \infty$ the second order Taylor approximation of the exponential function (84) can be used to get

$$\exp\left(-\tfrac{3}{2}(1-w)\int \Sigma_+^2 d\tau\right) \;=\; 1 + c_2^2 \tfrac{16u'(\bar{s})^2(1-w)}{(1-w-C)^2(1-w+C)} \exp\left(-\tfrac{3}{2}(1-w+C)\tau\right).$$

Since we are not interested in terms of higher order than ϵ we eliminated $O(\epsilon^2)$. Substituting this in equation (86) we see

$$H \;=\; H_0 \exp\left(-\tfrac{3}{2}(1+w)\tau\right)\left(1 + c_2^2 \tfrac{16u'(\bar{s})^2(1-w)}{(1-w-C)^2(1-w+C)} \exp\left(-\tfrac{3}{2}(1-w+C)\tau\right)\right) \tag{87}$$

which gives

$$H^{-1} \;=\; H_0^{-1} \exp\left(\tfrac{3}{2}(1+w)\tau\right)\left(1 + c_2^2 \tfrac{16u'(\bar{s})^2(1-w)}{(1-w-C)^2(1-w+C)} \exp\left(-\tfrac{3}{2}(1-w+C)\tau\right)\right)^{-1}.$$

The above equation can be simplified by using the approximation

$$\frac{1}{1+\epsilon} = 1 - \epsilon \quad \text{for small } \epsilon \tag{88}$$

hence ($\tau \to \infty$)

$$H^{-1} \;=\; H_0^{-1} \exp\left(\tfrac{3}{2}(1+w)\tau\right)\left(1 - c_2^2 \tfrac{16u'(\bar{s})^2(1-w)}{(1-w-C)^2(1-w+C)} \exp\left(-\tfrac{3}{2}(1-w+C)\tau\right)\right).$$

The next step is to transform τ back to the time t for which we need the formula

$$t = \int H^{-1} d\tau. \tag{89}$$

An easy integration with the constant of integration t_0 leads to the time t

$$t \;=\; \tfrac{2}{3H_0(1+w)} \exp\left(\tfrac{3}{2}(1+w)\tau\right) - \tfrac{32c_2^2 u'(\bar{s})^2(1-w)}{3H_0(1-w-C)^2(1-w+C)(2w-C)} \exp\left(\tfrac{3}{2}(2w-C)\tau\right) + t_0.$$

The constant of integration t_0 is set to zero because a translation in time does not change our results.

It is useful to have t of the form

$$t = \tfrac{2}{3(1+w)H_0} \exp\left(\tfrac{3}{2}(1+w)\tau\right)(1+x).$$

Thus we write

$$t \;=\; \tfrac{2}{3(1+w)H_0} \exp\left(\tfrac{3}{2}(1+w)\tau\right)\left(1 - \tfrac{16c_2^2 u'(\bar{s})^2(1-w)(1+w)}{(1-w-C)^2(1-w+C)(2w-C)} \exp\left(-\tfrac{3}{2}(1-w+C)\tau\right)\right). \tag{90}$$

We just investigate small deviations of time. That is why we suppose $\tau = \tau_0 + \Delta\tau$ with τ_0 being the solution of

$$t = \tfrac{2}{3(1+w)H_0} \exp\left(\tfrac{3}{2}(1+w)\tau_0\right)$$

given by

$$\tau_0 = \tfrac{2}{3(1+w)} \ln\left(\tfrac{3(1+w)H_0}{2} t\right) \tag{91}$$

and a small $\Delta\tau$. Substituting $\tau = \tau_0 + \Delta\tau$ in equation (90) we can solve for $\Delta\tau$. That is a long but straight forward calculation which gives (using again the approximations (84) and (88))

$$\Delta\tau = \tfrac{32c_2^2 u'(\bar{s})^2(1-w)}{3(1-w-C)^2(1-w+C)(2w-C)} \left(\tfrac{3(1+w)H_0}{2} t\right)^{-\frac{1-w+C}{1+w}}$$

and thus

$$\tau \;=\; \tfrac{2}{3(1+w)} \ln \tfrac{3(1+w)H_0}{2} t + \tfrac{32c_2^2 u'(\bar{s})^2(1-w)}{3(1-w-C)^2(1-w+C)(2w-C)} \left(\tfrac{3(1+w)H_0}{2} t\right)^{-\frac{1-w+C}{1+w}}. \tag{92}$$

All these calculations from above allow to transform the variable τ in g_{yy} (see equation (85)) into t. The first order approximation is

$$g_{yy} \;=\; \tilde{\tilde{g}}_{yy} \left(\tfrac{3(1+w)H_0}{2} t\right)^{\frac{4}{3(1+w)}} \left(1 - c_2 \tfrac{32u'(\bar{s})}{3(1-w)^2-3C^2} \left(\tfrac{3(1+w)H_0}{2} t\right)^{-\frac{1-w+C}{2(1+w)}}\right). \tag{93}$$

The next step is to calculate the other metric coefficients. Since $g_{yy} = g_{zz}$ the only missing metric coefficient is g_{xx}. The following formula will be used (equation (15) with $\nu = \mu = x$)

$$\partial_t g_{xx} = -2k_{xx}.$$

The use of equations (44), (45) and (52) leads to

$$\begin{aligned}\partial_t g_{xx} &= -2g_{xx}k_x^x \\ &= -2g_{xx}H(-1+2\Sigma_+)\end{aligned}$$

and transforming t into τ by the Hubble normalisation (53) one gets

$$\partial_\tau g_{xx} = -2g_{xx}(2\Sigma_+ - 1). \tag{94}$$

The same way we calculated g_{yy} we now can calculate g_{xx} which gives

$$g_{xx} = \tilde{\tilde{g}}_{xx}\left(\frac{3(1+w)H_0}{2}t\right)^{\frac{4}{3(1+w)}}\left(1+c_2\frac{64u'(\bar{s})(1-w+C)}{15(1-w-C)}\left(\frac{3(1+w)H_0}{2}t\right)^{-\frac{1-w+C}{2(1+w)}}\right) \tag{95}$$

with a constant $\tilde{\tilde{g}}_{xx}$.

Now we have found a first order approximation for the metric (93) and (95). This metric will be further discussed in section 6.5.2 and 6.5.3.

5.4.2 F as a nodal sink ($u'(\bar{s}) > 0$ and $u'(\bar{s}) \leq \frac{(1-w)^2}{32\bar{s}(1-2\bar{s})}$)

In this section we consider F as a nodal sink. The eigenvalues are real like in the first case thus we can use the accordant equations as before. The new Σ_+ of equation (80) cannot be simplified like in the above case. Nevertheless there are some restrictions of c_1 and c_2 but we keep our calculations as general as possible. Thus (80) is employed in equation (86). The approximation turns out to be the same as in the case discussed in the above section because the behaviour of Σ_+ is also like $e^{-\tau}$.

$$\begin{aligned}\int \Sigma_+^2 d\tau &= -c_1^2\frac{32u'(\bar{s})^2}{3(1-w+C)^2(1-w-C)}\exp\left(-\tfrac{3}{2}(1-w-C)\tau\right) \\ &\quad -\frac{64u'(\bar{s})^2c_1c_2}{3((1-w)^2-C^2)(1-w)}\exp\left(-\tfrac{3}{2}(1-w)\tau\right) \\ &\quad -c_2^2\frac{32u'(\bar{s})^2}{3(1-w-C)^2(1-w+C)}\exp\left(-\tfrac{3}{2}(1-w+C)\tau\right)\end{aligned}$$

In the first order approximation

$$\begin{aligned}\exp\left(-\tfrac{3}{2}(1-w)\int\Sigma_+^2 d\tau\right) &= 1+c_1^2\frac{16u'(\bar{s})^2(1-w)}{(1-w+C)^2(1-w-C)}\exp\left(-\tfrac{3}{2}(1-w-C)\tau\right) \\ &\quad +\frac{32u'(\bar{s})^2c_1c_2}{(1-w)^2-C^2}\exp\left(-\tfrac{3}{2}(1-w)\tau\right) \\ &\quad +c_2^2\frac{16u'(\bar{s})^2(1-w)}{(1-w-C)^2(1-w+C)}\exp\left(-\tfrac{3}{2}(1-w+C)\tau\right)\end{aligned}$$

holds. As this formula is very extensive we define new variables

$$\begin{aligned}A_1 &= c_1^2\frac{16u'(\bar{s})^2(1-w)}{(1-w+C)^2(1-w-C)} \\ A_2 &= c_1c_2\frac{32u'(\bar{s})^2}{(1-w)^2-C^2} \\ A_3 &= c_2^2\frac{16u'(\bar{s})^2(1-w)}{(1-w-C)^2(1-w+C)}\end{aligned}$$

which leads to (see equation (86) and emplying (88))

$$\begin{aligned} H^{-1} &= H_0^{-1}\exp\left(\tfrac{3}{2}(1+w)\tau\right)\left(1-A_1\exp\left(-\tfrac{3}{2}(1-w-C)\tau\right)\right. \\ &\left. -A_2\exp\left(-\tfrac{3}{2}(1-w)\tau\right)-A_3\exp\left(-\tfrac{3}{2}(1-w+C)\tau\right)\right). \end{aligned} \tag{96}$$

This H^{-1} can be used in $t=\int H^{-1}d\tau$ which gives an equation for t. Transformed into the form

$$t = \tfrac{2}{3(1+w)H_0}\exp\left(\tfrac{3}{2}(1+w)\tau\right)(1+x)$$

and a constant of integration equal to zero this equation reads

$$\begin{aligned} t &= \tfrac{2}{3(1+w)H_0}\exp\left(\tfrac{3}{2}(1+w)\tau\right)\left(1+\tfrac{A_1(1+w)}{2w+C}\exp\left(-\tfrac{3}{2}(1-w-C)\tau\right)\right. \\ &\left.+\tfrac{A_2(1+w)}{2}\exp\left(-\tfrac{3}{2}(1-w)\tau\right)+\tfrac{A_3(1+w)}{2w-C}\exp\left(-\tfrac{3}{2}(1-w+C)\tau\right)\right). \end{aligned}$$

The supposition $\tau=\tau_0+\Delta\tau$ with τ_0 like in equation (91) and $\Delta\tau$ very small may hold again. Analogous calculations (see last section) lead to

$$\begin{aligned} \tau &= \ln\left(\tfrac{3(1+w)H_0}{2}t\right)^{\frac{2}{3(1+w)}}-\tfrac{2A_1}{3(2w+C)}\left(\tfrac{3(1+w)H_0}{2}t\right)^{-\frac{1-w-C}{1+w}} \\ &-\tfrac{A_2}{3}\left(\tfrac{3(1+w)H_0}{2}t\right)^{-\frac{1-w}{1+w}}-\tfrac{2A_3}{3(2w-C)}\left(\tfrac{3(1+w)H_0}{2}t\right)^{-\frac{1-w+C}{1+w}} \end{aligned} \tag{97}$$

which give

$$\begin{aligned} g_{yy} &= \tilde{\tilde{g}}_{yy}\left(\tfrac{3(1+w)H_0}{2}t\right)^{\frac{4}{3(1+w)}}\left(1-c_1\tfrac{32u'(\bar{s})}{3(1-w)^2-3C^2}\left(\tfrac{3(1+w)H_0}{2}t\right)^{-\frac{1-w-C}{2(1+w)}}\right. \\ &\left.-c_2\tfrac{32u'(\bar{s})}{3(1-w)^2-3C^2}\left(\tfrac{3(1+w)H_0}{2}t\right)^{-\frac{1-w+C}{2(1+w)}}\right) \end{aligned} \tag{98}$$

with a constant $\tilde{\tilde{g}}_{yy}$.

Now found g_{yy} we search for the other metric coefficient g_{xx} by using equation (94). Integrating and approximating of that equation give ($\tilde{\tilde{g}}_{xx}$ is a constant)

$$\begin{aligned} g_{xx} &= \tilde{\tilde{g}}_{xx}\exp(2\tau)\left(1+c_1\tfrac{64u'(\bar{s})}{3(1-w+C)(1-w-C)}\exp\left(-\tfrac{3}{4}(1-w-C)\tau\right)\right. \\ &\left.+c_2\tfrac{64u'(\bar{s})}{3(1-w-C)(1-w+C)}\exp\left(-\tfrac{3}{4}(1-w+C)\tau\right)\right) \end{aligned}$$

and substituting τ by (97) the first order approximation of g_{xx} reads

$$\begin{aligned} g_{xx} &= \tilde{\tilde{g}}_{xx}\left(\tfrac{3(1+w)H_0}{2}t\right)^{\frac{4}{3(1+w)}}\left(1+c_1\tfrac{64u'(\bar{s})}{3(1-w+C)(1-w-C)}\left(\tfrac{3(1+w)H_0}{2}t\right)^{-\frac{1-w-C}{2(1+w)}}\right. \\ &\left.+c_2\tfrac{64u'(\bar{s})}{3(1-w-C)(1-w+C)}\left(\tfrac{3(1+w)H_0}{2}t\right)^{-\frac{1-w+C}{2(1+w)}}\right). \end{aligned} \tag{99}$$

The two coefficients (98) and (99) refer to the first meaningful case which will be examined in view of its observational relevance in section 6.5.2 and 6.5.3.

5.4.3 F as a spiral sink ($u'(\bar{s}) > \frac{(1-w)^2}{32\bar{s}(1-2\bar{s})}$)

In this last case the dynamical system (77) has complex eigenvalues. Hence the calculation of the metric coefficients is not as easy as in the cases above.

The first step is to transform Σ_+ by making use of

$$\alpha\cos(x) + \beta\sin(x) = \gamma\cos(x+\phi). \tag{100}$$

In this formula α, β and γ are constants, x is the argument of the trigonometric functions and ϕ is some kind of phase shift. Comparing this to equation (81) we find

$$\Sigma_+ = \gamma\exp\left(-\tfrac{3}{4}(1-w)\tau\right)\cos(\tilde{C}\tau+\phi) \tag{101}$$

with some constant γ and some phase shift ϕ. These two variables can be found by solving the equation

$$\frac{4u'(\bar{s})c_1(1-w)}{(1-w)^2+\tilde{C}^2}\cos(\tilde{C}\tau) - \frac{4u'(\bar{s})c_2\tilde{C}}{(1-w)^2+\tilde{C}^2}\sin(\tilde{C}\tau) = \gamma\cos(\tilde{C}\tau+\phi)$$

for γ and ϕ. Transforming

$$\gamma\cos(\tilde{C}\tau+\phi) = \gamma\cos(\phi)\cos(\tilde{C}\tau) - \gamma\sin(\phi)\sin(\tilde{C}\tau)$$

and comparing the coefficients we find

$$\phi = \arctan\left(\tfrac{c_2\tilde{C}}{c_1(1-w)}\right) \tag{102}$$

$$\gamma = \tfrac{4u'(\bar{s})c_1(1-w)}{(1-w)^2+\tilde{C}^2}\sqrt{1+\left(\tfrac{c_2\tilde{C}}{c_1(1-w)}\right)^2}. \tag{103}$$

That transformed Σ_+ (101) can now be substituted in (83) respectively (94) for whose solution we need the integral

$$\int \exp\left(-\tfrac{3}{4}(1-w)\tau\right)\cos(\tilde{C}\tau+\phi)d\tau.$$

Employing partial integration gives

$$\begin{aligned}\int \exp\left(-\tfrac{3}{4}(1-w)\tau\right)\cos(\tilde{C}\tau+\phi)d\tau \quad = \quad & -\tfrac{12(1-w)}{9(1-w)^2+16\tilde{C}^2}\exp\left(-\tfrac{3}{4}(1-w)\tau\right)\cos(\tilde{C}\tau+\phi) \\ & +\tfrac{16\tilde{C}^2}{9(1-w)^2+16\tilde{C}^2}\exp\left(-\tfrac{3}{4}(1-w)\tau\right)\sin(\tilde{C}\tau+\phi).\end{aligned}$$

We rewrite this term as

$$\int \exp\left(-\tfrac{3}{4}(1-w)\tau\right)\cos(\tilde{C}\tau+\phi)d\tau = \kappa\exp\left(-\tfrac{3}{4}(1-w)\tau\right)\cos(\tilde{C}\tau+\phi+\theta)$$

with the constants

$$\theta = \arctan\left(\tfrac{4\tilde{C}^2}{3(1-w)}\right)$$

$$\kappa = -\tfrac{12(1-w)}{9(1-w)^2+16\tilde{C}^2}\sqrt{1+\left(\tfrac{4\tilde{C}}{3(1-w)^2}\right)}.$$

Using this rewritten form we find a solutions of (83) and (94) as ($\tilde{\tilde{g_{yy}}}$ and $\tilde{\tilde{g_{xx}}}$ are the constants of integration)

$$g_{yy} = \tilde{\tilde{g_{yy}}} e^{2\tau}\left(1 + 2\gamma\kappa \exp\left(-\tfrac{3}{4}(1-w)\tau\right)\cos(\tilde{C}\tau + \phi + \theta)\right) \qquad (104)$$

$$g_{xx} = \tilde{\tilde{g_{xx}}} e^{2\tau}\left(1 - 4\gamma\kappa \exp\left(-\tfrac{3}{4}(1-w)\tau\right)\cos(\tilde{C}\tau + \phi + \theta)\right). \qquad (105)$$

Once more we need a transformation of τ into t. We gain this transformation using equation (86) for which we need the square of Σ_+.

$$\Sigma_+^2 = \gamma^2 \exp\left(-\tfrac{3}{2}(1-w)\right)\cos^2(\tilde{C}\tau + \phi)$$

In order to simplify this term we transform $\cos^2(x)$ to some not squared term.

$$\begin{aligned} \cos^2(x) - \sin^2(x) &= \cos(2x) \\ \cos^2(x) - 1 + \cos^2(c) &= \cos(2x) \\ \cos^2(x) &= \frac{\cos(2x) - 1}{2} \end{aligned}$$

This simplification leads to

$$\Sigma_+^2 = \gamma^2 \exp\left(-\tfrac{3}{2}(1-w)\tau\right)\tfrac{\cos(2\tilde{C}\tau + 2\phi) - 1}{2}$$

and thus

$$\begin{aligned} \int \Sigma_+^2 d\tau &= \int \tfrac{\gamma^2}{2}\exp\left(-\tfrac{3}{2}(1-w)\tau\right)\cos(2\tilde{C}\tau + 2\phi) - \tfrac{\gamma^2}{2}\exp\left(-\tfrac{3}{2}(1-w)\tau\right)d\tau \qquad (106) \\ &= \frac{\gamma^2}{3(1-w)}\exp\left(-\tfrac{3}{2}(1-w)\tau\right) + \int \frac{\gamma^2}{2}\exp\left(-\tfrac{3}{2}(1-w)\tau\right)\cos(2\tilde{C}\tau + 2\phi)d\tau. \end{aligned}$$

The integral on the right hand side will be integrated separately using partial integration. (As the constants do not have any effect on the integration they are left aside.)

$$\begin{aligned} \int \exp\left(-\tfrac{3}{2}(1-w)\tau\right)\cos(2\tilde{C}\tau + 2\phi)d\tau &= -\tfrac{2}{3(1-w)}\exp\left(-\tfrac{3}{2}(1-w)\tau\right)\cos(2\tilde{C}\tau + 2\phi) \\ &- \int \tfrac{2}{3(1-w)}\exp\left(-\tfrac{3}{2}(1-w)\tau\right)2\tilde{C}\sin(2\tilde{C}\tau + 2\phi)d\tau \\ &= -\tfrac{2}{3(1-w)}\exp\left(-\tfrac{3}{2}(1-w)\tau\right)\cos(2\tilde{C}\tau + 2\phi) \\ &\quad + \tfrac{8\tilde{C}}{9(1-w)^2}\exp\left(-\tfrac{3}{2}(1-w)\tau\right)\sin(2\tilde{C}\tau + 2\phi) - \\ &\quad - \tfrac{16\tilde{C}^2}{9(1-w)^2}\int \exp\left(-\tfrac{3}{2}(1-w)\tau\right)\cos(2\tilde{C}\tau + 2\phi)d\tau \end{aligned}$$

Hence

$$\begin{aligned} \int \exp\left(-\tfrac{3}{2}(1-w)\tau\right)\cos(2\tilde{C}\tau + 2\phi)d\tau &= -\tfrac{6(1-w)}{9(1-w)^2 + 16\tilde{C}^2}\exp\left(-\tfrac{3}{2}(1-w)\tau\right)\cos(2\tilde{C}\tau + 2\phi) \\ &\quad + \tfrac{8\tilde{C}}{9(1-w)^2 + 16\tilde{C}^2}\exp\left(-\tfrac{3}{2}(1-w)\tau\right)\sin(2\tilde{C}\tau + 2\phi). \end{aligned}$$

As this is also a linear combination of sine and cosine terms it can be transformed to

$$\int \exp\left(-\tfrac{3}{2}(1-w)\tau\right)\cos(2\tilde{C}\tau+2\phi)d\tau = \hat{\gamma}\exp\left(-\tfrac{3}{2}(1-w)\tau\right)\cos(2\tilde{C}\tau+2\phi+\psi)$$

with a constant $\hat{\gamma}$ and a new phase shift ψ.

$$\begin{aligned}\psi &= \arctan(\tfrac{4\tilde{C}}{3(1-w)})\\ \hat{\gamma} &= -\tfrac{6(1-w)}{9(1-w)^2+16\tilde{C}^2}\sqrt{1+\tfrac{16\tilde{C}^2}{9(1-w)^2}}\end{aligned}$$

Substituting these new results in equation (106) one finds

$$\int \Sigma_+^2 d\tau = \tfrac{\gamma^2}{3(1-w)}\exp\left(-\tfrac{3}{2}(1-w)\tau\right) + \tfrac{\gamma^2\hat{\gamma}}{2}\exp\left(-\tfrac{3}{2}(1-w)\tau\right)\cos(2\tilde{C}\tau+2\phi+\psi).$$

In equation (86) we need the term

$$\begin{aligned}\exp\left(-\tfrac{3}{2}(1-w)\textstyle\int\Sigma_+^2 d\tau\right) &= \exp\Big(-\tfrac{\gamma^2}{2}\exp\left(-\tfrac{3}{2}(1-w)\tau\right)\\ &\quad -\tfrac{3\gamma^2\hat{\gamma}(1-w)}{4}\exp\left(-\tfrac{3}{2}(1-w)\tau\right)\cos(2\tilde{C}\tau+2\phi+\psi)\Big)\end{aligned}$$

We find again that $\int\Sigma_+^2 d\tau \to 0$ if $\tau\to\infty$ which allows us to make use of the first order approximation (84).

$$\begin{aligned}\exp\left(-\tfrac{3}{2}(1-w)\textstyle\int\Sigma_+^2 d\tau\right) &= 1-\tfrac{\gamma^2}{2}\exp\left(-\tfrac{3}{2}(1-w)\tau\right)\\ &\quad -\tfrac{3\gamma^2\hat{\gamma}(1-w)}{4}\exp\left(-\tfrac{3}{2}(1-w)\tau\right)\cos(2\tilde{C}\tau+2\phi+\psi).\end{aligned}$$

This simplified term is now used in equation (86) which gives

$$\begin{aligned}H &= H_0\exp\left(-\tfrac{3}{2}(1+w)\tau\right)\Big(1-\tfrac{\gamma^2}{2}\exp\left(-\tfrac{3}{2}(1-w)\tau\right)\\ &\quad -\tfrac{3\gamma^2\hat{\gamma}(1-w)}{4}\exp\left(-\tfrac{3}{2}(1-w)\tau\right)\cos(2\tilde{C}\tau+2\phi+\psi)\Big).\end{aligned}\tag{107}$$

The next step is to find t via $t=\int H^{-1}d\tau$. Hence we need

$$\begin{aligned}H^{-1} &= H_0^{-1}\exp\left(\tfrac{3}{2}(1+w)\tau\right)\Big(1-\tfrac{\gamma^2}{2}\exp\left(-\tfrac{3}{2}(1-w)\tau\right)\\ &\quad -\tfrac{3\gamma^2\hat{\gamma}(1-w)}{4}\exp\left(-\tfrac{3}{2}(1-w)\tau\right)\cos(2\tilde{C}\tau+2\phi+\psi)\Big)^{-1}.\end{aligned}$$

To simplify this we can use approximation (88)

$$\begin{aligned}H^{-1} &= H_0^{-1}\exp\left(\tfrac{3}{2}(1+w)\tau\right)\Big(1+\tfrac{\gamma^2}{2}\exp\left(-\tfrac{3}{2}(1-w)\tau\right)\\ &\quad +\tfrac{3\gamma^2\hat{\gamma}(1-w)}{4}\exp\left(-\tfrac{3}{2}(1-w)\tau\right)\cos(2\tilde{C}\tau+2\phi+\psi)\Big)\end{aligned}$$

and thus

$$\begin{aligned}t &= \int H_0^{-1}\exp\left(\tfrac{3}{2}(1+w)\tau\right)+\tfrac{\gamma^2}{2H_0}e^{3w\tau}\\ &\quad +\tfrac{3\gamma^2\hat{\gamma}(1-w)}{4H_0}e^{3w\tau}\cos(2\tilde{C}\tau+2\phi+\psi)d\tau.\end{aligned}\tag{108}$$

The last part of the integral is solved separately with partial integration which leads via straight forward calculations as above to

$$\begin{aligned}\int \tfrac{3\gamma^2\hat{\gamma}(1-w)}{4H_0}e^{3w\tau}\cos(2\tilde{C}\tau+2\phi+\psi)d\tau &= \tfrac{3\gamma^2\hat{\gamma}(1-w)}{4H_0}\tfrac{3w}{9w^2+4\tilde{C}^2}e^{3w\tau}\cos(2\tilde{C}\tau+2\phi+\psi)\\ &\quad +\tfrac{3\gamma^2\hat{\gamma}(1-w)}{4H_0}\tfrac{2\tilde{C}}{9w^2+4\tilde{C}^2}e^{3w\tau}\sin(2\tilde{C}\tau+2\phi+\psi)\\ &= \hat{\hat{\gamma}}e^{3w\tau}\cos(2\tilde{C}\tau+2\phi+\psi+\delta)\end{aligned}$$

with a new constant $\hat{\hat{\gamma}}$ and another phase shift δ.

$$\begin{aligned}\delta &= -\arctan(\tfrac{2\tilde{C}}{3w}) && (109)\\ \hat{\hat{\gamma}} &= \tfrac{3\gamma^2\hat{\gamma}(1-w)}{4H_0}\tfrac{3w}{9w^2+4\tilde{C}^2}\sqrt{1+\tfrac{4\tilde{C}^2}{9w^2}} && (110)\end{aligned}$$

In the following we set $\alpha = 2\phi+\psi+\delta$. If we make use of this new variable and calculate the missing integrals from (108) we gain

$$t = \tfrac{2}{3H_0(1+w)}\exp\left(\tfrac{3}{2}(1+w)\tau\right) + \tfrac{\gamma^2}{6H_0 w}\exp(3w\tau) + \hat{\hat{\gamma}}\exp(3w\tau)\cos(2\tilde{C}\tau+\alpha)$$

with a constant of integration set equal to zero (because it is just a translation in time and thus does not have any effect on our calculations). Once more we transform t to the form

$$t = \tfrac{2}{3(1+w)H_0}\exp\left(\tfrac{3}{2}(1+w)\tau\right)(1+x).$$

Hence we write

$$\begin{aligned}t &= \tfrac{2}{3(1+w)H_0}\exp\left(\tfrac{3}{2}(1+w)\tau\right)\Big(1+\tfrac{(1+w)\gamma^2}{4w}\exp\left(-\tfrac{3}{2}(1-w)\tau\right)+\\ &\quad +\tfrac{3\hat{\hat{\gamma}}H_0(1+w)}{2}\exp\left(-\tfrac{3}{2}(1-w)\tau\right)\cos(2\tilde{C}\tau+\alpha)\Big).\end{aligned}$$

Like in the above two sections we suppose again $\tau = \tau_0 + \Delta\tau$. Employing (91) we get

$$\begin{aligned}1 &= \exp\left(\tfrac{3}{2}(1+w)\Delta\tau\right)\Big(1+\tfrac{(1+w)\gamma^2}{4w}\exp\left(-\tfrac{3}{2}(1-w)\tau_0\right)\exp\left(-\tfrac{3}{2}(1-w)\Delta\tau\right)+ && (111)\\ &\quad +\tfrac{3H_0\hat{\hat{\gamma}}(1+w)}{2}\exp\left(-\tfrac{3}{2}(1-w)\tau_0\right)\exp\left(-\tfrac{3}{2}(1-w)\Delta\tau\right)\cos\Big(2\tilde{C}(\tau_0+\Delta\tau)+\alpha\Big)\Big).\end{aligned}$$

The term $\exp\left(-\frac{3}{2}(1-w)\tau_0\right)$ in this equation can be calculated by substituting τ_0 by (91) which leads to

$$\exp\left(-\tfrac{3}{2}(1-w)\tau_0\right) = \left(\tfrac{3(1+w)H_0}{2}t\right)^{-\frac{1-w}{1+w}}.$$

In equation (111) remains a cosine term with a compounded argument. For simplification we use a first order Taylor approximation (ϵ is small) for the cosine term

$$\cos(x+\epsilon) = \cos(x) - \epsilon\sin(x)$$

which gives

$$\begin{aligned}\cos(2\tilde{C}(\tau_0+\Delta\tau)+\alpha) &= \cos(2\tilde{C}\tau_0+\alpha)-2\tilde{C}\Delta\tau\sin(2\tilde{C}\tau_0+\alpha)\\ &= \cos\left(2\tilde{C}\ln\left((\tfrac{3(1+w)H_0}{2}t)^{\frac{2}{3(1+w)}}\right)+\alpha\right)-\\ &\quad -2\tilde{C}\Delta\tau\sin\left(2\tilde{C}\ln\left((\tfrac{3(1+w)H_0}{2}t)^{\frac{2}{3(1+w)}}\right)+\alpha\right).\end{aligned}$$

Making use of these two found relations equation (111) reads

$$\begin{aligned}1 &= \exp\left(\tfrac{3}{2}(1+w)\Delta\tau\right)\Bigg(1+\tfrac{(1-w)\gamma^2}{4w}\left(\tfrac{3(1+w)H_0}{2}t\right)^{-\frac{1-w}{1+w}}\exp\left(-\tfrac{3}{2}(1-w)\Delta\tau\right)\\ &\quad+\tfrac{3H_0\hat{\tilde{\gamma}}(1+w)}{2}\left(\tfrac{3(1+w)H_0}{2}t\right)^{-\frac{1-w}{1+w}}\exp\left(-\tfrac{3}{2}(1-w)\Delta\tau\right)\Bigg[\cos\left(2\tilde{C}\ln\left((\tfrac{3(1+w)H_0}{2}t)^{\frac{2}{3(1+w)}}\right)+\alpha\right)\\ &\quad-2\tilde{C}\Delta\tau\sin\left(2\tilde{C}\ln\left((\tfrac{3(1+w)H_0}{2}t)^{\frac{2}{3(1+w)}}\right)+\alpha\right)\Bigg]\Bigg).\end{aligned}$$

Employing the two approximations (84) and (88), cancelling the ones and leaving away terms of quadratic order and higher the equation we find is

$$\begin{aligned}-\tfrac{3}{2}(1+w)\Delta\tau &= \tfrac{(1-w)\gamma^2}{4w}\left(\tfrac{3(1+w)H_0}{2}t\right)^{-\frac{1-w}{1+w}}\\ &\quad+\tfrac{3H_0\hat{\tilde{\gamma}}(1+w)}{2}\left(\tfrac{3(1+w)H_0}{2}t\right)^{-\frac{1-w}{1+w}}\cos\left(2\tilde{C}\ln\left((\tfrac{3(1+w)H_0}{2}t)^{\frac{2}{3(1+w)}}\right)+\alpha\right).\end{aligned}$$

The next step is to solve this equation for $\Delta\tau$.

$$\begin{aligned}\Delta\tau &= -\tfrac{(1-w)\gamma^2}{6w(1+w)}\left(\tfrac{3(1+w)H_0}{2}t\right)^{-\frac{1-w}{1+w}}\\ &\quad-H_0\hat{\tilde{\gamma}}\left(\tfrac{3(1+w)H_0}{2}t\right)^{-\frac{1-w}{1+w}}\cos\left(2\tilde{C}\ln\left((\tfrac{3(1+w)H_0}{2}t)^{\frac{2}{3(1+w)}}\right)+\alpha\right)\end{aligned}$$

Hence

$$\begin{aligned}\tau &= \ln\left(\tfrac{3(1+w)H_0}{2}t\right)^{\frac{2}{3(1+w)}}-\tfrac{(1-w)\gamma^2}{6w(1+w)}\left(\tfrac{3(1+w)H_0}{2}t\right)^{-\frac{1-w}{1+w}}\\ &\quad-H_0\hat{\tilde{\gamma}}\left(\tfrac{3(1+w)H_0}{2}t\right)^{-\frac{1-w}{1+w}}\cos\left(2\tilde{C}\ln\left((\tfrac{3(1+w)H_0}{2}t)^{\frac{2}{3(1+w)}}\right)+\alpha\right).\end{aligned}\tag{112}$$

All these longsome calculations led us to a relation between τ and t thus now we are able to search for g_{xx} and g_{yy} depending on t like in the first and second case by transforming τ of the equations (104) and (105) into t. The use of the above equation gives as first order approximation

$$\begin{aligned}g_{yy} &= \tilde{\tilde{g}}_{yy}\left(\tfrac{3(1+w)H_0}{2}t\right)^{\frac{4}{3(1+w)}}(1+ \\ &\quad+2\gamma\kappa\left(\tfrac{3(1+w)H_0}{2}t\right)^{-\frac{1-w}{2(1+w)}}\cos\left(\tilde{C}\ln(\tfrac{3(1+w)H_0}{2}t)^{\frac{2}{3(1+w)}}+\phi+\theta\right)\Big)\end{aligned}\tag{113}$$

$$\begin{aligned}g_{xx} &= \tilde{\tilde{g}}_{xx}\left(\tfrac{3(1+w)H_0}{2}t\right)^{\frac{4}{3(1+w)}}(1- \\ &\quad-4\gamma\kappa\left(\tfrac{3(1+w)H_0}{2}t\right)^{-\frac{1-w}{2(1+w)}}\cos\left(\tilde{C}\ln(\tfrac{3(1+w)H_0}{2}t)^{\frac{2}{3(1+w)}}+\phi+\theta\right)\Big).\end{aligned}\tag{114}$$

Thus we have also a first order approximation for the metric of F as a spiral sink which will also be examined to its observational relevance and accordance to the age of the universe gained from observational astronomy.

6 Interpretation of the different metrics and experimental view

Up to now our considerations were purely theoretical. In the following we will discuss what the theoretical results tell us about the universe and what implication they have. Moreover we will compare our theoretical considerations and calculations to observational data which has been compiled in the last decades by several scientists. We will find out whether our calculations fit to the experimental found data or not.

6.1 Hubble constant

Before discussing the different models we will elucidate the Hubble constant which will help us later on to find out about the age of the universe.
In the year 1929 Edwin Hubble found a correlation between the distance and the recessional velocity of distant objects, see [12]. It is a linear relation

$$v = H_0 \; d$$

with a recessional velocity v, distance d of the object and the Hubble constant H_0. The recessional velocity can be gained from the red shift of a star's spectrum which can be determined easily by comparing the spectrum of the star to labour spectra.

There are three main effects which cause red shift: the peculiar motion of a star, the expansion of the universe and gravitation. The first two are due to the *Doppler effect* which says that the wavelength of a moving object changes. If the source nears, one observes shorter wavelength which is blue shift and if the wave is emitted by a source moving away the wavelength is longer and red shift is observed. Gravitation can also cause red shift which is due to time dilation. (For detailed explanation see [32] p.79 ff)

First calculations and observations of Hubble (he used several measured data of V. Slipher) allowed him to state the formula (see [13])

$$v = \frac{d(parsec)}{1790} \tag{115}$$

with an uncertainty of 10%. That formula led to an age of 0.55 billion years. This first result was actually not right because it was known that even the earth was older (and the universe has to be at least as old as the earth). The following years were full of controversies and discussions of the expansion of the universe. A lot of research has been done and corrections have been applied. In the year 1956 Humason, Mayall and Sandage found a new value of the Hubble constant of $180km/s/Mpc$ [14]. Just two years later Sandage reduced the value to $75km/s/Mpc$ [27]. In the following years several observations were carried out and several adjustment values have been found. The latest researches of August 2012 by Freedman et al. [10] gave a value of

$$H_0 = 74.3 \pm 2.1km/s/Mpc \tag{116}$$

with a systematic uncertainty. In the following we will use this constant which is the Hubble parameter at present time to find out the age of the universe corresponding to the different models via the function of the Hubble parameter.

6.2 Another way to determine the age of the universe

There are several other ways to determine the age of the universe, explaining all of these would be beyond the scope of this work. Therefore we will just describe the most popular one whose results can be read up [6].

When trying to determine the age of the universe it is useful to observe globular clusters. The theory assumes that the universe has to be at least as old as the oldest stars. The objects in globular clusters have low metallicity and their distribution is nearly spherical about the galactic centre. That is why these objects are seen as to be one of the oldest in our universe. To ascertain the age of stars astronomers often use the *Hertzsprung-Russell diagrams* (HRD). This diagram was invented by Hertzsprung in the year 1913 and puts the luminosity (or absolute magnitudes) in relation to their spectral types. In this diagram there is a main sequence turn-off which is considered to be the best stellar clock. Thus if we know when a star passes the main sequence turn-off we know its age. A lot of examinations were made to determine the age of stars belonging to globular clusters. A grave problem with this investigations is defining the error. What is known is that the two most sensitive quantities are the distance and the chemical composition. These uncertainties can give an error of about 22%. Examinations with this method give a minimum age of the universe of 11 Gyr. Since the error of such outcomes is quite big the range of the age of the universe is denoted as $11 - 21$ Gyr. To get the results of the extremal values a lot of assumptions have to be true. That is why it seems more realistic to find the age of the universe according to this method in a range of $13 - 17$ Gyr.

The results of this section serve as reference for the following ones. Once found the age of the universe via Hubble constant according to the different cosmological models we will compare the result to the one of this section and see whether they are in agreement or not.

6.3 FLRW metric

In section 4.3 we found a solution of the Einstein equations satisfying the Cosmological Principle (i.e. there is no specially favoured position in the universe or in other words that all positions in the universe are basically equal).
The most general metric which satisfies the Cosmological Principle is often referred to as *Robertson-Walker* metric and is

$$d\tau = -dt + a(t)\frac{dx^2 + dy^2 + dz^2}{(1 + \frac{1}{4}k(x^2 + y^2 + z^2))^2}.$$

Different signs of k give different geometries for the universe namely

- $sign\ k = -1$ corresponds to an open universe
- $sign\ k = 0$ corresponds to a flat universe (the FLRW model we discussed)
- $sign\ k = 1$ corresponds to a closed universe.

For further information about this different types see e.g. [19] p.722 ff.

In the theoretical section we treated the Cosmological Principle as a fact. Actually we know that the Cosmological Principle does not apply in detail since our solar system is not homogeneous. Even outside of our solar system the universe seems inhomogeneous because there are a lot of different stars. Several stars constitute a galaxy and several galaxies in turn constitute clusters. Even these clusters are grouped together as clusters of galaxy clusters. Hence the universe does not seem homogeneous even on scales of Mpc. Thus the question remains: "Why is this model so successful?".

An important reason why the Cosmological Principle model is used frequently is: it is very simple. We have got very little data from observational astronomy. If we try to model this data with anisotropy or other weaker assumptions than the Cosmological Principle, a lot of functions remain undetermined. Nevertheless the question is: "In which way does the Cosmological Principle fit to the real universe?"

As indicated before, the universe seems locally very inhomogeneous. Nevertheless on large scales (scales larger than the diameter of clusters of galaxies i.e. 10^8 to 10^9 light years) it is not. The first to find out that the universe is nearly isotropic were Patridge and Wilkinson [23] in 1967. They detected and measured the cosmic blackbody radiation near the celestial equator over one year. What they found was an anisotropy of maximal 0.2% which demonstrates that the universe is nearly isotropic (the little anisotropy is due to the initial stages of the universe). Maddox et al. [16] - [18] have also found indications for the isotropy of the universe in the year 1990. Moreover they showed the homogeneity of our universe using a catalogue of several galaxies. Maddox et al. defined a galaxy clustering correlation function and thus were able to demonstrate that over whole depths of the catalogue the hypothesis of homogeneity seems to correspond well with the function. These researches justify to treat the Cosmological Principle as a fact because indeed it is a very good approximation of the universe.

In the section 6.3 we found an equation for the Hubble parameter in a FLRW model (see (72)). Now we use the experimental determined H_0 which gives us the value of the Hubble parameter at present time to find out the age of the universe according to this model. Transforming equation (72) results in

$$t_0 = \frac{2}{3(1+w)H_0}$$

and substituting the value of H_0 given by (116) gives

$$t_0 = \frac{8.78}{1+w} \; \textit{billion years}.$$

Since $w \in (-1/3, 1)$ the above equation gives a range of the age of

$$t_0 \in (4.39, 13.17) \; \textit{billion years}$$

which is plotted in figure 5.

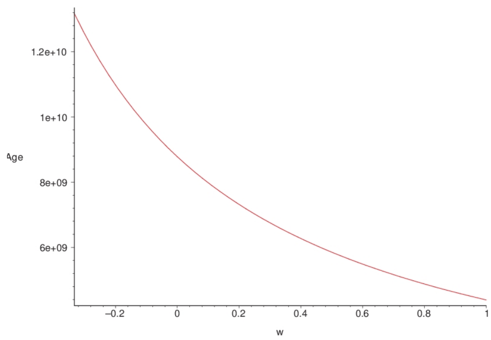

Figure 5: The age [years] of the universe according to the FLRW model depending on different values of w.

Comparing this result to section 6.2 where a range of the age of the universe of $13-17$ years was found we may conclude that the universe is neither radiation dominated (w=1/3) nor matter dominated (w=0). Thus a negative w is needed to get a result which coincides with section 6.2.

6.4 Kasner metric

In this section observational relevance of the Kasner equations, discussed theoretically in section 4.4, is examined. Below a brief summary following [19] section 30.2 is given. We write the Kasner metric in a more general way

$$-dt^2 + t^{2p_1}dx^2 + t^{2p_2}dy^2 + t^{2p_3}dz^2$$

with the p_i fulfilling the so called *Kasner relations*

$$\sum_i p_i = 1 \qquad \text{and} \qquad \sum_i p_i^2 = 1.$$

These two relations define a circle in $\mathbb{R}^3$. The extremal values of the p_i give the solutions we found in section 4.4. In the mentioned section the first solution, the Taub solution, refers to a flat universe (because the curvature tensor vanishes) with a coordinate singularity at $t = 0$. On the contrary the second solution is a non-flat solution and has a physical singularity at $t = 0$ (see [29] p.178).

The Kasner model is very asymmetric but just in a few degrees of freedom. Moreover it is homogeneous but not isotropic. In the frame of Kasner the spatial manifold can either be $\mathbb{R}^3$ or T^3 which is the threedimensional torus. If the manifold is assumed to be $\mathbb{R}^3$ there is another symmetry which is rotation in (y,z) plane whereas if T^3 is supposed it is a LRS model.

The vacuum cosmological model refers to an expanding universe (but of an anisotropicly expanding universe) because the volume element which is given in a Kasner model by

$$\sqrt{-det(g_{\mu\nu})} = t$$

is increasing with time. The fact that the expansion is anisotropic can be seen easily. An observer parallel to the x-axis finds an expansion proportional to t^{p_1}. Parallel to the y-axis an expansion proportional to t^{p_2} is found. Since in general $p_1 \neq p_2$ the expansion is anisotropic. Furthermore the model is contracting in one direction if the belonging p_i is nonpositive which leads to a blue shift in this direction (see section 6.3 for explanation of the Doppler effect). However up to now there are no observations which could demonstrate such a blue shift which might lead to the conclusion that the Kasner model is not the right model for the universe.

In section 5.3.1 we found a function for the Hubble parameter (63) which holds for the Taub solution as well as for the non-flat LRS solution. If the experimental found H_0 (which is the Hubble parameter at present time) of section 6.1 is assumed to be correct the age of the universe is found as limit ($w = 1$) of the result of the last section namely

$$Age = 4.39 \text{ billion years.}$$

This value is a lot smaller than the results of section 6.2. That may indicate that the Kasner model does not fit the universe very well.

6.5 LRS Bianchi type I with anisotropic matter

In this section we will compare the observational achievements to the results we gained n section 5. The points T_b, T_a, Q_b and Q_a refer to Kasner solutions which have been discussed in the above section 6.4. Moreover the only fixed point in the interior F refers to the Friedmann solution which has also been examined in the prior, see section 6.3. What remains are the solutions at the points R_b and R_a of section 5.3.3 as well as the metric in the environment of F which has been established in section 5.4.

6.5.1 Hubble parameter at R_a and R_b

First we will start with examining the function for the Hubble parameter at the equilibrium points R_b respectively R_a which depend on the anisotropy parameter β.

In section 5.3.3 we found the function of the Hubble parameter at R_b as (65)

$$H(t) = \frac{2}{3(1 + w + \beta^2(1 - w))t}$$

and at R_a see equation (69)

$$H(t) = \frac{2}{3\left(1 + w + \beta^2/4(1 - w)\right)t}.$$

These two functions turn into the function for the Hubble parameter of the Friedmann metric (see section 6.1) if $\beta = 0$ which is compulsory since $\beta = 0$ represents isotropy. As the anisotropy parameter β appears in these functions we infer that the age of the universe according to this results depend on anisotropy. Nevertheless the anisotropy parameter is according to experiments (see section 6.3) very small. Even in the theoretical section 5.3.3 we found limitation for β namely

- $\beta \in (-1, 1)$ for R_b
- and $\beta \in (-2, 2)$ for R_a.

Taking into account this constrictions we find an age of the universe depending on β and w as shown in figure 6. (Once more we use H_0 of section 6.1 as the present Hubble parameter.)

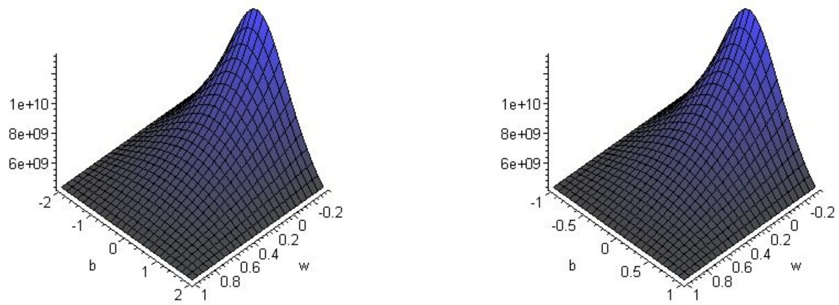

(a) R_a (b) R_b

Figure 6: The possible solutions for the age [years] for different values of w and β.

Thus we conclude: If the absolute value of the anisotropy parameter increases, the value of w has to decrease to obtain an age of the universe in agreement with section 6.2. Hence this result may also indicate that the universe is not very anisotropic (because $w > -1/3$).

6.5.2 Hubble parameter in the environment of F

The last part is the discussion of the solutions in the environment of F for which we found a first order approximation in section 5.4. Like in the theoretical section we have to distinguish between the three cases of F being a saddle, a nodal sink or a spiral sink. Since the solutions of F as a saddle only tend to F in one characteristic direction the solutions of F being a nodal sink or a spiral sink are more meaningful. Nevertheless we start with the case of F as a saddle to get the main idea using the simplest case.

- F as a saddle

  Firstly we search for the Hubble parameter if F is a saddle. In section 5.4.1 we found the Hubble parameter depending on τ (equation (87)). As we search for H depending on t we transform τ into t via (92) which leads in first order approximation to

$$H(t) = \frac{2}{3(1+w)t}\left(1 + \frac{16(1-w)u'(\bar{s})^2(2+6w-3C)}{3(1-w-C)^2(1-w+C)(2w-C)}\left(\frac{3(1+w)H_0}{2}t\right)^{-\frac{1-w+C}{1+w}}\right). \qquad (117)$$

Note that this equation is an approximation and only holds for big t. That is why we cannot just solve this equation for t and use the H_0 of section 6.1 to find out about the age of the universe because the equation does not hold for small times i.e. in the beginning of the universe.

The second term in brackets has to be small in comparison to 1 to get a good approximation. In the following we suppose the absolute value of this term to be smaller than 0.2 and find out from which time t on the approximation holds.

What is also missing is a function for the undetermined $u(s)$ which can be gained (in the simplest way) by making a linear ansatz

$$u(s) = as + b$$

with two constants a and b. Employing the equations (39) one finds

$$u(s) = \tfrac{3(1-w)\beta}{2} s + w - \tfrac{(1-w)\beta}{2} \tag{118}$$

and thus

$$u'(\bar{s}) = \tfrac{3(1-w)\beta}{2}. \tag{119}$$

Moreover we can solve $u(\bar{s}) = w$ for $\bar{s}$. Employing $u(s)$ as given in (118) leads to

$$\bar{s} = \tfrac{1}{3}.$$

Using the linear ansatz of $u(s)$ (118) and its deductions the constant C of equation (78) reads

$$C = \sqrt{(1-w)^2 - \tfrac{16(1-w)\beta}{3}}. \tag{120}$$

All we have gained so far is inserted into equation (117) which allows us to search for the time t from which on that equation is a good approximation.

The condition for F being a saddle is $u'(\bar{s}) < 0$ which implies (see (119)) $\beta < 0$. The found times t depending on β and w from which on (117) is a good approximation are plotted in the following figure 7.

In figure 7 we find some singularities which refer to the zeros of the denominator of the second bracket term of (117) which are

$$\begin{aligned}(w,b) &= (1,b)\\ (w,b) &= (w,0)\\ (w,b) &= (w, \tfrac{3(-1+2w+3w^2)}{16(w-1)}).\end{aligned} \tag{121}$$

Leaving beside the extremal values we find an estimation for the validity of (117) of $10^{10} - 10^{11}$ years. Now we compare $H(t)$ of equation (117) to the one we found for the FLRW, see equation (72). In Appendix B $H(t)$ is plotted for different values

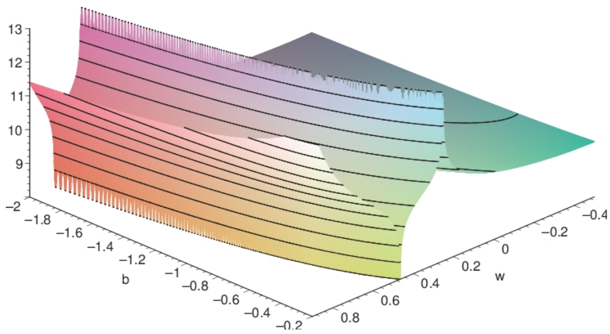

Figure 7: F as a saddle: The time $[log_{10}(\text{years})]$ from which on $H(t)$ of (117) is a good approximation.

of β and w (F as a saddle see figure 11 and 13). In these figures can be seen that all $H(t)$ have similar behaviour and the ones with $\beta \neq 0$ converge to that of the FLRW model - this convergence is quite quickly since there is hardly any difference between the values of our model independent of β and those of the FLRW model for ages bigger than 10^{11} years. The difference between the $H(t)$ with variable β and the $H(t)$ of the FLRW model are shown in figure 12 for $w = 1/3$ and in figure 14 for $w = 0$. In plot 12b one finds a difference lower than 1.2 $km/s/Mpc$ from $5 \cdot 10^{10}$ years on and in figure 14b even lower than 0.2 $km/s/Mpc$.

- F as a nodal sink

The second and first meaningful case is F as a nodal sink. Appropriate calculations using the results (96) and (97) of section 5.4.2 give the first order approximation

$$\begin{aligned} H(t) &= \tfrac{2}{3(1+w)t}\left(1+\tfrac{16c_1^2u'(\bar{s})^2(1-w)(1+3w+C)}{(1-w+C)^2(1-w-C)(2w+C)}\left(\tfrac{3(1+w)H_0}{2}t\right)^{-\frac{1-w-C}{1+w}}\right. \\ &\quad +\tfrac{16c_1c_2u'(\bar{s})^2(3+w)}{(1-w)^2-C^2}\left(\tfrac{3(1+w)H_0}{2}t\right)^{-\frac{1-w}{1+w}} \\ &\quad \left.+\tfrac{16c_2^2u'(\bar{s})^2(1-w)(1+3w-C)}{(1-w-C)^2(1-w+C)(2w-C)}\left(\tfrac{3(1+w)H_0}{2}t\right)^{-\frac{1-w+C}{1+w}}\right). \end{aligned} \tag{122}$$

We adopt the same assumptions for $u(s)$ as in the previous section. Thus we can substitute u' of equation (119) and C of (120) into equation (122). To get a nodal sink $u'(\bar{s})$ has to fulfil $u'(\bar{s}) > 0$ and $u'(\bar{s}) \leq \frac{(1-w)^2}{32\bar{s}(1-2\bar{s})}$ which leads (see (119)) to restrictions of β namely $\beta > 0$ and $\beta \leq \frac{3(1-w)}{16}$.

In the following we examine different directions of the phase portrait.

  - The first direction to be considered is $c_1 = 1$ and $c_2 = 0$. Thus $H(t)$ of equation (122) simplifies to

$$H(t) = \tfrac{2}{3(1+w)t}\left(1+\tfrac{16c_1^2u'(\bar{s})^2(1-w)(1+3w+C)}{(1-w+C)^2(1-w-C)(2w+C)}\left(\tfrac{3(1+w)H_0}{2}t\right)^{-\frac{1-w-C}{1+w}}\right). \tag{123}$$

Again we search for the time t from which on the above approximation holds (we assume as in the previous section that the approximation is reliable if the absolute value of the second term in brackets is smaller than 0.2.) That time is plotted in figure 8.

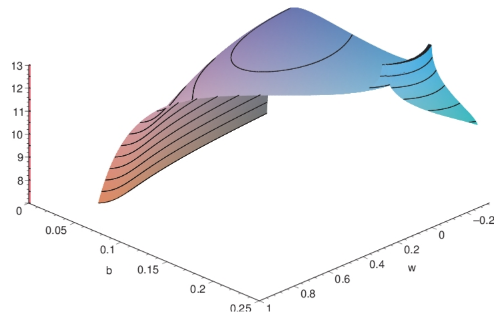

Figure 8: F as a nodal sink with $c_1 = 1$ and $c_2 = 0$: The time [log_{10}(years)] from which on $H(t)$ of (123) is a valid approximation.

The singularities in that figure are due to the zeros of the denominator of the second term which are the same as is the previous section see (121). In this case we find that (depending on the parameters β and w) the made approximation starts to hold for times of about $10^{11} - 10^{12}$ years. Moreover the approximation holds for smaller times if the anisotropy parameter is smaller.

Now we compare the found $H(t)$ of equation (123) to the one we found for the FLRW model (equation (72)). In Appendix B, for F as a nodal sink with $c_1 = 1$ and $c_2 = 0$ in figure 15 and 17 , plots of $H(t)$ with different values of β and w are shown. As above all different functions of $H(t)$ converge to the one of the FLRW model. Nevertheless in this case more time has to pass until the varied models give identical values for $H(t)$ than in the case of F as a saddle. Moreover the difference of the $H(t)$ with distinct β and the $H(t)$ of the FLRW model is plotted in the figures 16 and 18. If $w = 1/3$ we find about $3 \cdot 10^{11}$ years have to pass until the difference is lower than 1 $km/s/Mpc$ and if $w = 0$ even $3 \cdot 10^{12}$ years have to pass. This is ten times (for $w = 1/3$) and hundred times (for $w = 0$) the time which has to pass to find such a difference in the case of F as a saddle.

– The second direction to give attention to is $c_1 = 0$ and $c_2 = 1$ for which (122) reduces to

$$H(t) \quad = \quad \frac{2}{3(1+w)t}\left(1 + \frac{16c_2^2 u'(\bar{s})^2(1-w)(1+3w-C)}{(1-w-C)^2(1-w+C)(2w-C)}\left(\frac{3(1+w)H_0}{2}t\right)^{-\frac{1-w+C}{1+w}}\right). \quad (124)$$

The times t depend on β and w from which on this equation is reliable (the approximation is legitimate if the absolute value of the second term in brackets is smaller than 0.2) are illustrated in figure 9.

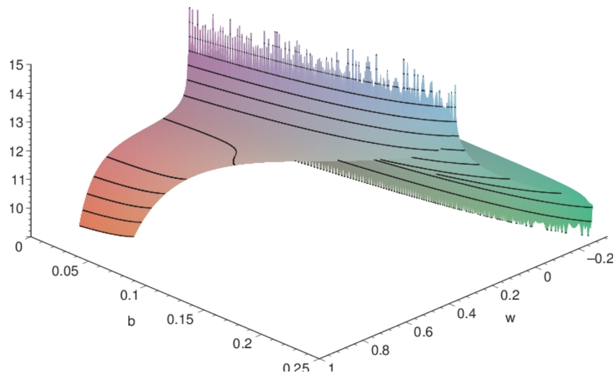

Figure 9: F as a nodal sink for $c_1 = 0$ and $c_2 = 1$: The time l[log_{10}(years)] from which on $H(t)$ of (124) is a valid approximation.

Once more we find singularities at (121) - the part in the middle which seems a little scraggy is due to the resolution capacity of the software Maple and just indicates a singularity. In the above figure 9 one sees that the time from which on the approximation (124) holds is lower if β nears 0 or w nears $-1/3$. The corresponding $H(t)$ of this section with different values of β and w are again shown in Appendix B, figures 19 and 21. Furthermore the difference of the $H(t)$ with variable values of β and $H(t)$ of the FLRW model is shown in figure 20 for $w = 1/3$ and in figure 22 for w=0. The same convergence as in the above case is found. Now the convergence is faster again - similar to the case of F as a saddle. If $w = 0$ we find that the difference between the $H(t)$ with different β and the $H(t)$ of the FLRW model is smaller than 1 $km/s/Mpc$ at times of about $8 \cdot 10^{10}$ years whereas if $w = 1/3$ about $3 \cdot 10^{11}$ years have to pass .

- F as a spiral sink

The last case is F as a spiral sink which refers to the Hubble function of (107). Employing τ of equation (112) in that equation we find the first order approximation

$$\begin{aligned} H(t) &= \tfrac{2}{3(1+w)t}\left(1 - \left(\tfrac{\gamma^2}{2} + \tfrac{(1-w)\gamma^2}{6w(1+w)}\right.\right. \\ &\quad + \tfrac{3\gamma^2\hat{\gamma}(1-w)}{4}\cos\left(2\tilde{C}\ln\left(\tfrac{3(1+w)H_0}{2}t\right)^{\frac{2}{3(1+w)}} + 2\phi + \psi\right) \\ &\quad \left.\left. + H_0\hat{\hat{\gamma}}\cos\left(2\tilde{C}\ln\left(\tfrac{3(1+w)H_0}{2}t\right)^{\frac{2}{3(1+w)}} + \alpha\right)\right)\left(\tfrac{3(1+w)H_0}{2}t\right)^{-\frac{1-w}{1+w}}\right). \end{aligned} \tag{125}$$

Evaluating the variables δ and $\hat{\hat{\gamma}}$ of (109) and (110) we divide by w which is not possible if $w = 0$. Thus we conduct the same calculation we made in section 5.4.3

substituting $w = 0$ and get

$$\begin{aligned}\delta_{w=0} &= \frac{\pi}{2}\\ \hat{\hat{\gamma}}_{w=0} &= \frac{3\gamma^2\hat{\gamma}}{8\tilde{C}H_0}\end{aligned}$$

and

$$\begin{aligned}H(t)_{w=0} &= \tfrac{2}{3t}\Big(1 - \tfrac{\gamma^2}{3H_0 t}\Big(1 + \ln\big(\tfrac{3H_0}{2}t\big)^{\frac{2}{3}}\Big) - \tfrac{\gamma^2\hat{\gamma}}{2H_0 t}\cos\Big(2\tilde{C}\ln\big(\tfrac{3H_0}{2}t\big)^{\frac{2}{3}} + 2\phi + \psi\Big)\\ &\quad -H_0\hat{\hat{\gamma}}\cos\Big(2\tilde{C}\ln\big(\tfrac{3H_0}{2}t\big)^{\frac{2}{3}} + \alpha\Big)\Big). \qquad (126)\end{aligned}$$

We use the same ansatz for $u(s)$ as above (see (118)). Furthermore we have a reduction of possible values of β again. In this case u' has to fulfil $u' > \frac{(1-w)^2}{32\bar{s}(1-2\bar{s})}$ which gives via (119) the restriction $\beta > \frac{3(1-w)}{16}$.

Like in the previous section we will also discuss special directions of the phase portrait namely $c_1 = 1$ and $c_2 = 0$ on the one hand and $c_1 = 0$ and $c_2 = 1$ on the other hand.

- $c_1 = 1$ and $c_2 = 0$

  Firstly we look into the direction of c_1. We search again for the time t from which on the above approximations of $H(t)$ (125) and (126) are justified. Since now the Hubble function is very complex the software (Maple) used is not able to produce a plot like in the above two cases. Hence we just examine some explicit matter models. Namely $w = 1/3$ which represents radiation and $w = 0$ which stands for dust. Several values of the time for the different matter models with variable β are listed in table 1.

  This table tells us to expect the approximation to hold for values of about $10^{10} - 10^{11}$ years. Thus we can compare the $H(t)$ of this section to the one of the FLRW model starting at 10^{10} years (see figure 23 and 25 in Appendix B). In these figures we see that in the beginning (at times of 10^{10} years) the $H(t)$ are diverse but all near the one of the FLRW model at higher ages of about 10^{12} years. The plotted difference can be seen in figure 24 for $w = 1/3$ and in figure 26 for $w = 0$. In this case the convergence of the $H(t)$ is different to the ones above because now the $H(t)$ do not converge monotonically but rather converge oscillating (best to see in figure 26c). The differences are smaller than 1 $km/s/Mpc$ at about 10^{11} years in both cases even though for $w = 1/3$ the convergence is a little faster.

w	β	Time [years]
1/3	0.15	$0.66 \cdot 10^{10}$
	0.35	$6.25 \cdot 10^{10}$
	0.55	$5.45 \cdot 10^{10}$
	0.75	$4.56 \cdot 10^{10}$
	0.95	$3.99 \cdot 10^{10}$
	1.15	$3.61 \cdot 10^{10}$
	1.35	$3.34 \cdot 10^{10}$
	1.55	$3.14 \cdot 10^{10}$
	1.75	$2.99 \cdot 10^{10}$
	1.95	$2.87 \cdot 10^{10}$
	2.15	$2.77 \cdot 10^{10}$
	2.35	$2.69 \cdot 10^{10}$
	2.55	$2.62 \cdot 10^{10}$
	2.75	$2.57 \cdot 10^{10}$
	2.95	$2.53 \cdot 10^{10}$
	3.15	$2.49 \cdot 10^{10}$
	3.35	$2.46 \cdot 10^{10}$
	3.55	$2.44 \cdot 10^{10}$
	3.75	$2.42 \cdot 10^{10}$
	3.95	$2.42 \cdot 10^{10}$

w	β	Time [years]
0	0.19	$0.51 \cdot 10^{10}$
	0.39	$3.89 \cdot 10^{10}$
	0.59	$4.40 \cdot 10^{10}$
	0.79	$4.10 \cdot 10^{10}$
	0.99	$4.26 \cdot 10^{10}$
	1.19	$9.19 \cdot 10^{10}$
	1.39	$8.38 \cdot 10^{10}$
	1.59	$7.75 \cdot 10^{10}$
	1.79	$7.25 \cdot 10^{10}$
	1.99	$6.86 \cdot 10^{10}$
	2.19	$6.54 \cdot 10^{10}$
	2.39	$6.28 \cdot 10^{10}$
	2.59	$6.07 \cdot 10^{10}$
	2.79	$5.90 \cdot 10^{10}$
	2.99	$5.77 \cdot 10^{10}$
	3.19	$5.67 \cdot 10^{10}$
	3.39	$5.61 \cdot 10^{10}$
	3.59	$5.61 \cdot 10^{10}$
	3.79	$5.71 \cdot 10^{10}$
	3.99	$6.28 \cdot 10^{10}$

Table 1: Times from which on (125) respectively (126) with $c_1 = 1$ and $c_2 = 0$ is a valid approximation: for different values of β and w.

– $c_1 = 0$ and $c_2 = 1$

The second case is the direction of c_2 for which we have to modify the variables ϕ of equation (102) and γ of equation (103) to avoid division by zero.

$$\begin{aligned} \phi_{c_1=0} &= \frac{\pi}{2} \\ \gamma_{c_1=0} &= -\frac{4u'(\bar{s})c_2(1+w)}{(1-w)^2+\tilde{C}^2} \end{aligned}$$

This time as well, Maple cannot produce a plot. Thus we consider again special matter models to get the time from which on (125) and (126) (using the new variables $\phi_{c_1=0}$ and $\gamma_{c_1=0}$) are reliable. Some of these values are listed in the following table 2.

As in the previous section the approximation starts to hold for times of 10^{10} to 10^{11} years. The comparison of the $H(t)$ of this section to the one of the FLRW model is displayed in figure 27 and 29, in Appendix B. We find nearly the same results as in the former section namely: at times of 10^{10} years the $H(t)$ with variable β are very distinct but for times of 10^{12} years the functions seem to overlap. The differences between the $H(t)$ of our model and the one

w	β	Time [years]	w	β	Time [years]
1/3	0.15	$9.66 \cdot 10^{10}$	0	0.19	$4.43 \cdot 10^{8}$
	0.35	$- \cdot 10^{10}$		0.39	$2.46 \cdot 10^{11}$
	0.55	$2.01 \cdot 10^{10}$		0.59	$1.03 \cdot 10^{11}$
	0.75	$1.88 \cdot 10^{10}$		0.79	$7.67 \cdot 10^{10}$
	0.95	$1.85 \cdot 10^{10}$		0.99	$6.55 \cdot 10^{10}$
	1.15	$1.87 \cdot 10^{10}$		1.19	$5.92 \cdot 10^{10}$
	1.35	$1.94 \cdot 10^{10}$		1.39	$5.54 \cdot 10^{10}$
	1.55	$2.11 \cdot 10^{10}$		1.59	$5.29 \cdot 10^{10}$
	1.75	$2.54 \cdot 10^{10}$		1.79	$5.16 \cdot 10^{10}$
	1.95	$3.30 \cdot 10^{10}$		1.99	$5.16 \cdot 10^{10}$
	2.15	$3.60 \cdot 10^{10}$		2.19	$0.32 \cdot 10^{10}$
	2.35	$3.69 \cdot 10^{10}$		2.39	$7.69 \cdot 10^{10}$
	2.55	$3.69 \cdot 10^{10}$		2.59	$7.70 \cdot 10^{10}$
	2.75	$3.66 \cdot 10^{10}$		2.79	$7.55 \cdot 10^{10}$
	2.95	$3.61 \cdot 10^{10}$		2.99	$7.36 \cdot 10^{10}$
	3.15	$3.55 \cdot 10^{10}$		3.19	$7.17 \cdot 10^{10}$
	3.35	$3.49 \cdot 10^{10}$		3.39	$6.98 \cdot 10^{10}$
	3.55	$3.43 \cdot 10^{10}$		3.59	$6.81 \cdot 10^{10}$
	3.75	$3.37 \cdot 10^{10}$		3.79	$6.65 \cdot 10^{10}$
	3.95	$3.31 \cdot 10^{10}$		3.99	$6.50 \cdot 10^{10}$

Table 2: Times from which on (125) respectively (126) with $c_1 = 0$ and $c_2 = 1$ is a valid approximation: for different values of β and w.

of the FLRW model are plotted in figure 28 and 30. Like in the above case we find oscillations of the differences which are smaller than 1 $km/s/Mpc$ at times of 10^{11} years.

6.5.3 The age of the universe numerical approach

In the last section we examined the Hubble function according to the metric of the environment of F. Since the approximated Hubble function does not hold for small times we cannot invert it to search for the age of the universe. Thus the software Mathematica was used to solve the dynamical system (54), (55) and (59) for different values of w and β (with $u(s)$ of (118)) numerically. Then we employed the values of $H(\tau)$ to find the age of the universe via (53). Different phase portraits of (54) and (55) for future times are shown in Appendix A. Considering these portraits with opposite direction of the arrows we find the behaviour of the past times and thus the equilibrium points. The convergence of the functions towards an equilibrium point (most of the time Q_a) is in general quickly i.e. $\tau = -3$ to -5. Hence we integrated the function $1/H(t)$ numerically to this value and then used Σ_+ of the equilibrium point. In the following table 3 different results of the numeric calculations with different initial conditions are listed.

$\Sigma_+(0) = 0.1,\ s(0) = 0.3$		
w	β	age [years]
1/3	0	$6.46 \cdot 10^9$
	0.1	$6.46 \cdot 10^9$
	0.2	$6.46 \cdot 10^9$
	1	$6.50 \cdot 10^9$
	-1	$6.44 \cdot 10^9$
0	0	$7.99 \cdot 10^9$
	0.1	$8.00 \cdot 10^9$
	0.2	$8.02 \cdot 10^9$
	1	$8.33 \cdot 10^9$
	-1	$7.97 \cdot 10^9$
-0.2	0	$9.01 \cdot 10^9$
	0.1	$9.03 \cdot 10^9$
	0.2	$9.05 \cdot 10^9$
	1	$9.69 \cdot 10^9$
	-1	$9.07 \cdot 10^9$

$\Sigma_+(0) = 0.6,\ s(0) = 0.2$		
w	β	age [years]
1/3	0	$5.21 \cdot 10^9$
	0.1	$5.21 \cdot 10^9$
	0.2	$5.20 \cdot 10^9$
	1	$5.20 \cdot 10^9$
	-1	$5.25 \cdot 10^9$
0	0	$5.50 \cdot 10^9$
	0.1	$5.49 \cdot 10^9$
	0.2	$5.48 \cdot 10^9$
	1	$5.43 \cdot 10^9$
	-1	$5.60 \cdot 10^9$
-0.2	0	$5.64 \cdot 10^9$
	0.1	$5.63 \cdot 10^9$
	0.2	$5.61 \cdot 10^9$
	1	$5.53 \cdot 10^9$
	-1	$5.79 \cdot 10^9$

$\Sigma_+(0) = 0.9,\ s(0) = 0.1$		
w	β	age [years]
1/3	0	$4.58 \cdot 10^9$
	0.1	$4.58 \cdot 10^9$
	0.2	$4.57 \cdot 10^9$
	1	$4.53 \cdot 10^9$
	-1	$4.68 \cdot 10^9$
0	0	$4.63 \cdot 10^9$
	0.1	$4.62 \cdot 10^9$
	0.2	$4.61 \cdot 10^9$
	1	$4.56 \cdot 10^9$
	-1	$4.82 \cdot 10^9$
-0.2	0	$4.65 \cdot 10^9$
	0.1	$4.64 \cdot 10^9$
	0.2	$4.63 \cdot 10^9$
	1	$4.56 \cdot 10^9$
	-1	$4.90 \cdot 10^9$

Table 3: The age of the universe according to the metric of the environment of F for different values of β and w and variable initial conditions.

In this table we find that the age of the universe seems to increase if w decreases. Moreover if we start the considerations far away from F the anisotropy parameter β has hardly any effect on the age of the universe. What is also interesting is that in the case of $\Sigma_+(0) = 0.1$ and $s(0) = 0.3$ with $w = 0$ or $w = -0.2$ the ages increase with increasing absolute value of β. This seems to be some numeric mistake since we know that the anisotropy parameter is small but need a higher age for coincidence with section 6.

7 Discussion and outlook

As mentioned in the first section a cosmological constant can be added to the Einstein equations (7) in the way

$$R_{\mu\nu} - \frac{1}{2} R g_{\mu\nu} + \Lambda g_{\mu\nu} = T_{\mu\nu} \tag{127}$$

with Λ the cosmological constant. Since the term with the cosmological constant can be moved to the right hand side of this equation it can be interpreted as an extra energy momentum tensor due to some kind of extra energy called dark energy. The existence of such an energy would accelerate the universe. In all our considerations above we set the cosmological constant equal to zero. Was this suitable or was it a mistake?

Einstein who was convinced that the universe was static introduced the cosmological constant to find such a solution to his equations. After the observations of Hubble which tell that the universe is expanding the cosmological constant was removed. Nevertheless new measurements of the acceleration of the universe lead to a cosmological model $\Lambda \neq 0$. In the year 2011 S. Perlmutter, B.P. Schmidt and A. Riess were given the Nobel Prize in Physics *for the discovery of the accelerating expansion of the Universe through observations of distant supernovae.*

A nonzero cosmological constant in our model above would be represented by $w = -1$. We did not allow $w < -1/3$ because such matter sources violate energy conditions (for details see [4]). Nevertheless we have seen in the sections 6.3, 6.5.1 and 6.5.3 that using a negative w gives better coincidence of the age of the universe according to our calculations and to that according to the globular cluster method of section 6.2. Thus we may think of the universe as to be filled with different types of matter e.g. dust, radiation, dark energy and others to get a combined matter model which gives a negative average value of w.

Moreover we considered w to be constant which is according to scientists not true. The early universe was filled with different matter than the one the universe is filled nowadays (also in other composition). Thus a model with a time dependent w would be needed to get a more accurate approximation of our universe.

8 Appendix A

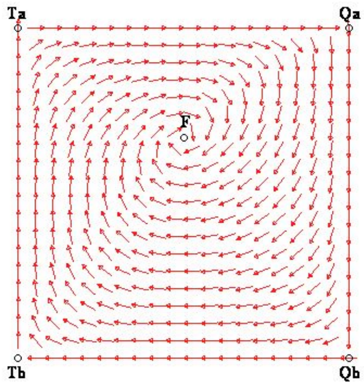

(a) $w = -0.2, \beta = 2.5$

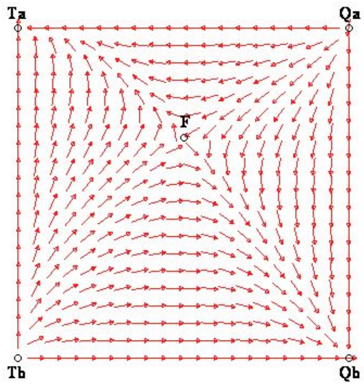

(b) $w = -0.2, \beta = -2.5$

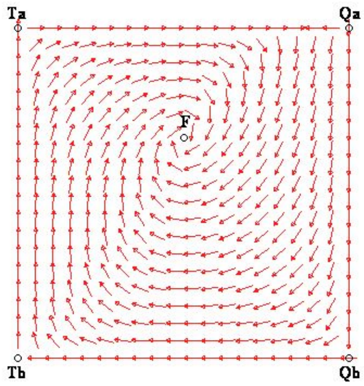

(c) $w = -0.2, \beta = 1.5$

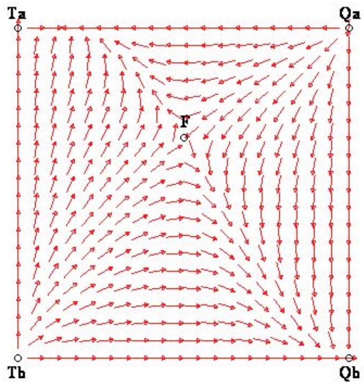

(d) $w = -0.2, \beta = -1.5$

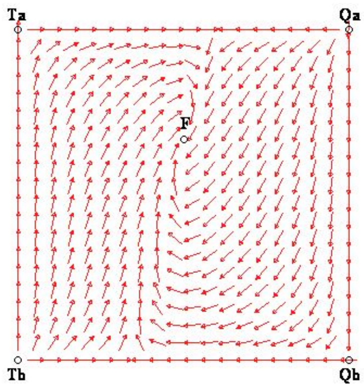

(e) $w = -0.2, \beta = 1/3$

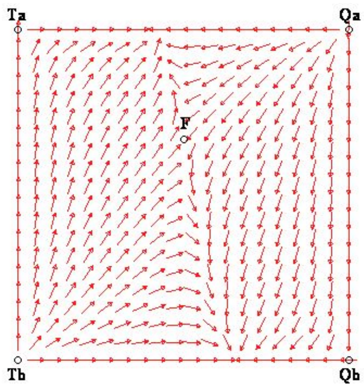

(f) $w = -0.2, \beta = -1/3$

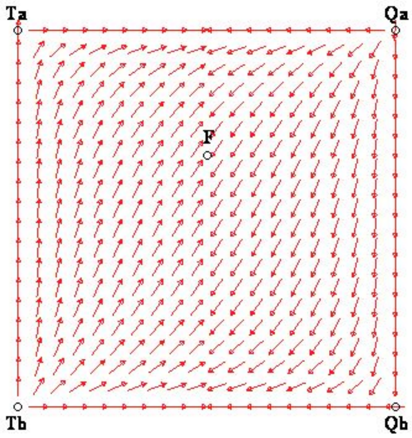

(g) $w = -0.2$,$\beta = 0$

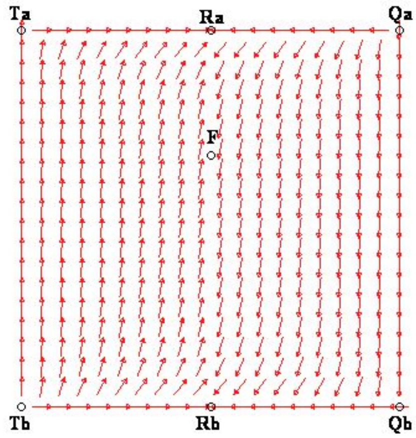

(h) $w = 2/3$,$\beta = 0$

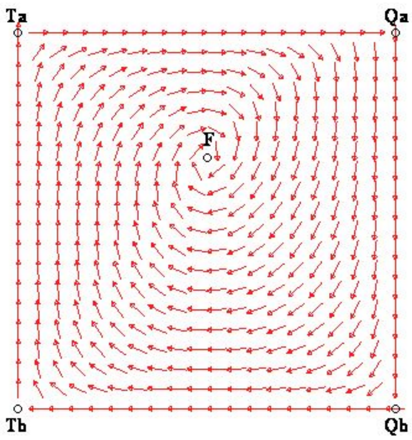

(i) $w = 1/3$,$\beta = 2.5$

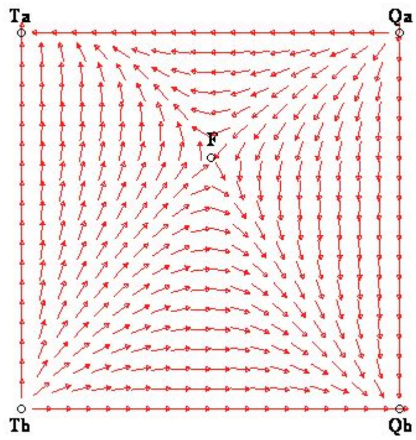

(j) $w = 1/3$,$\beta = -2.5$

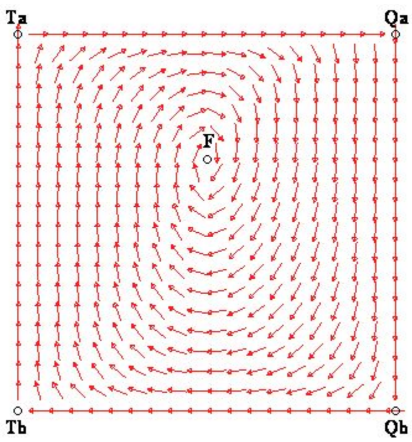

(k) $w = 2/3$,$\beta = 2.5$

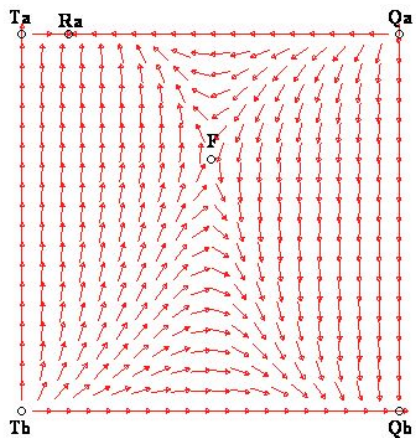

(l) $w = 2/3$,$\beta = -1.5$

Figure 10: Phase portraits of different values of w and β.

9 Appendix B

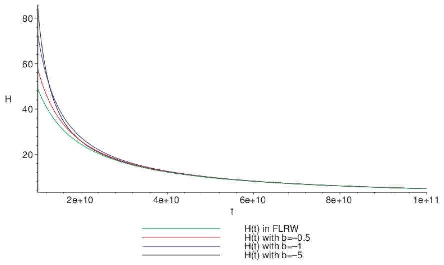

(a) $H(t)$ [km/s/Mpc] in the range of $10^{10} - 10^{11}$ years

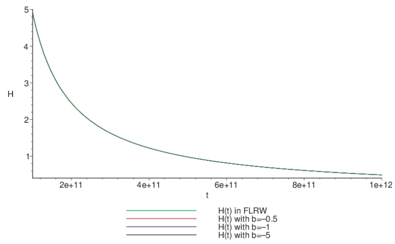

(b) H(t) [km/s/Mpc] in the range of $10^{11} - 10^{12}$ years

Figure 11: F as a saddle: H(t) for different values of β and $w = 1/3$ which represents radiation.

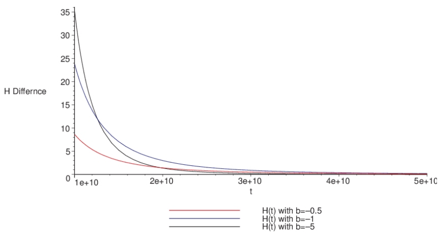

(a) Difference of $H(t)$ [km/s/Mpc] in the range of $10^{10} - 5 \cdot 10^{10}$ years

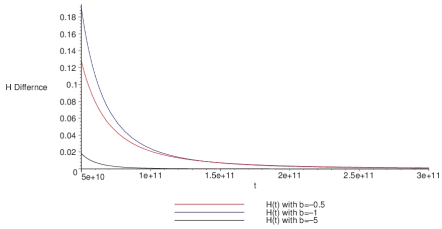

(b) Difference of $H(t)$ [km/s/Mpc] in the range of $5 \cdot 10^{10} - 3 \cdot 10^{11}$ years

Figure 12: F as a saddle: Difference of H(t) with different β and the $H(t)$ of the FLRW solution for $w = 1/3$ which represents radiation.

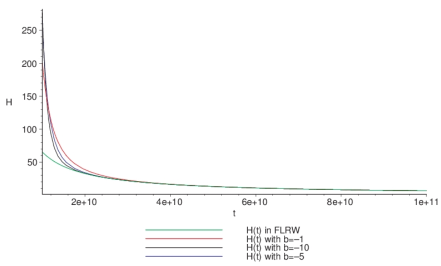

(a) $H(t)$ [km/s/Mpc] in the range of $10^{10} - 10^{11}$ years

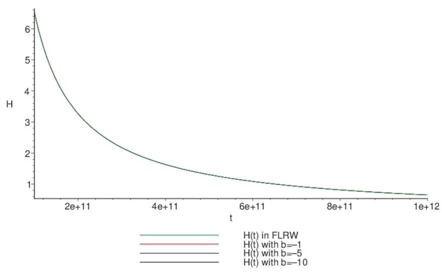

(b) H(t) [km/s/Mpc] in the range of $10^{11} - 10^{12}$ years

Figure 13: F as a saddle: H(t) for different values of β and $w = 0$ which represents dust.

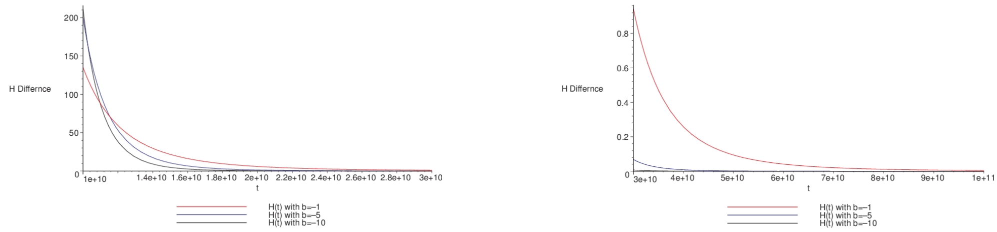

(a) Difference of $H(t)$ [km/s/Mpc] in the range of $10^{10} - 3 \cdot 10^{10}$ years

(b) Difference of $H(t)$ [km/s/Mpc] in the range of $3 \cdot 10^{10} - \cdot 10^{11}$ years

Figure 14: F as a saddle: Difference of H(t) with different β and the $H(t)$ of the FLRW solution for $w = 0$ which represents dust.

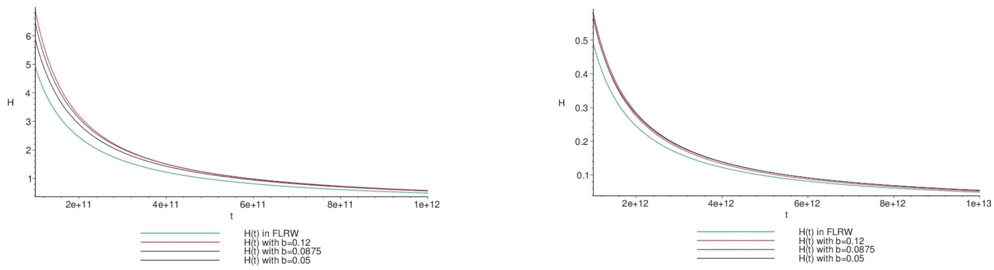

(a) $H(t)$ [km/s/Mpc] in the range of $10^{11} - 10^{12}$ years

(b) $H(t)$ [km/s/Mpc] in the range of $10^{12} - 10^{13}$ years

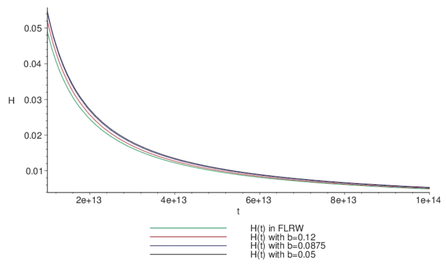

(c) $H(t)$ [km/s/Mpc] in the range of $10^{13} - 10^{14}$ years

Figure 15: F as a nodal sink with $c_1 = 1$ and $c_2 = 0$: H(t) for different values of β and $w = 1/3$ which represents radiation.

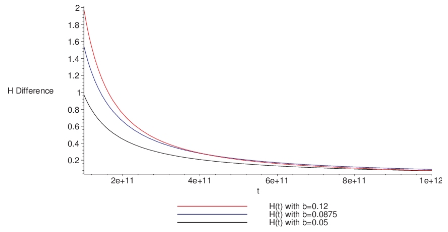

(a) Difference of $H(t)$ [km/s/Mpc] in the range of $10^{11} - 10^{12}$ years

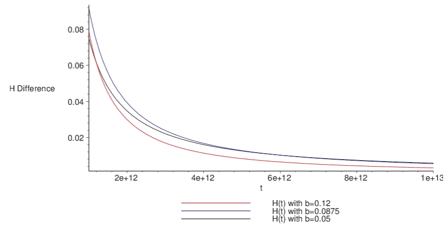

(b) Difference of $H(t)$ [km/s/Mpc] in the range of $10^{12} - 10^{13}$ years

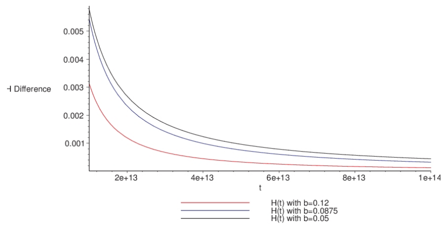

(c) Difference of $H(t)$ [km/s/Mpc] in the range of $10^{13} - 10^{14}$ years

Figure 16: F as a nodal sink with $c_1 = 1$ and $c_2 = 0$: Difference of $H(t)$ for different values of β and $H(t)$ of the FLRW model for $w = 1/3$ which represents radiation.

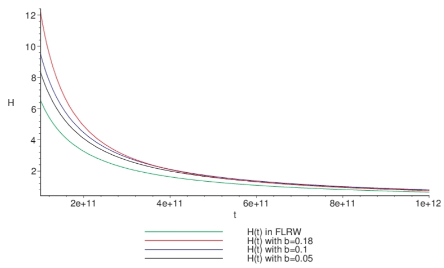

(a) $H(t)$ [km/s/Mpc] in the range of $10^{11} - 10^{12}$ years

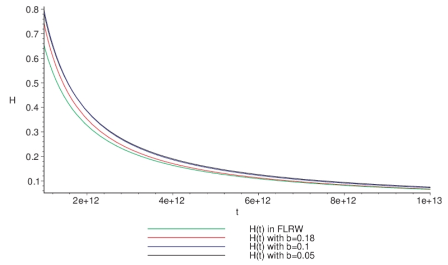

(b) $H(t)$ [km/s/Mpc] in the range of $10^{12} - 10^{13}$ years

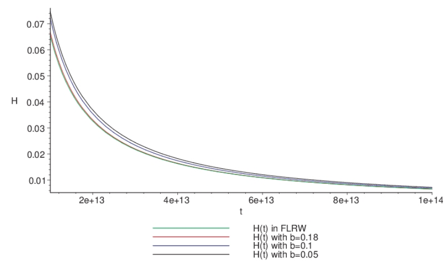

(c) $H(t)$ [km/s/Mpc] in the range of $10^{13} - 10^{14}$ years

Figure 17: F as a nodal sink with $c_1 = 1$ and $c_2 = 0$: H(t) for different values of β and $w = 0$ which represents dust.

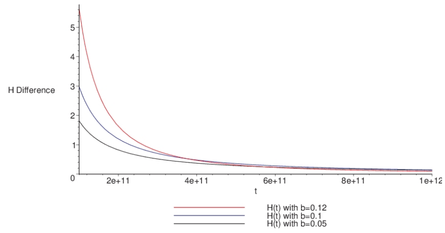

(a) Difference of $H(t)$ [km/s/Mpc] in the range of $10^{11} - 10^{12}$ years

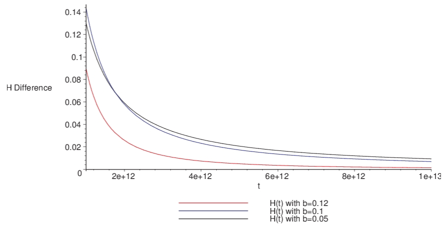

(b) Difference of $H(t)$ [km/s/Mpc] in the range of $10^{12} - 10^{13}$ years

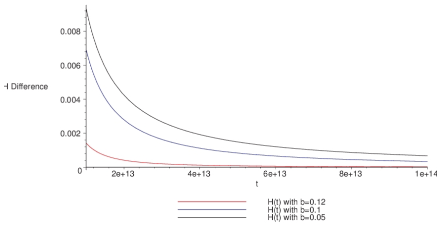

(c) Difference of $H(t)$ [km/s/Mpc] in the range of $10^{13} - 10^{14}$ years

Figure 18: F as a nodal sink with $c_1 = 1$ and $c_2 = 0$: Difference of $H(t)$ for different values of β and $H(t)$ of the FLRW model for $w = 0$ which represents dust.

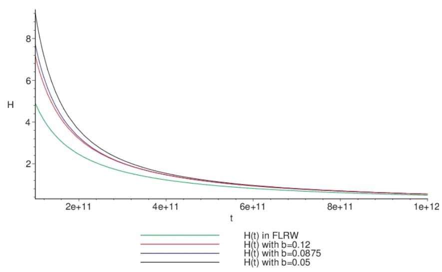

(a) $H(t)$ [km/s/Mpc] in the range of $10^{11} - 10^{12}$ years

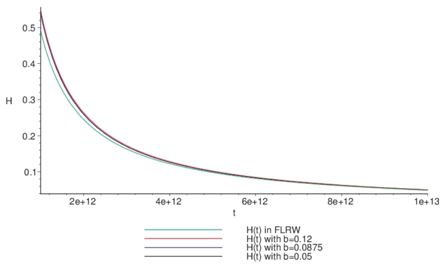

(b) $H(t)$ [km/s/Mpc] in the range of $10^{12} - 10^{13}$ years

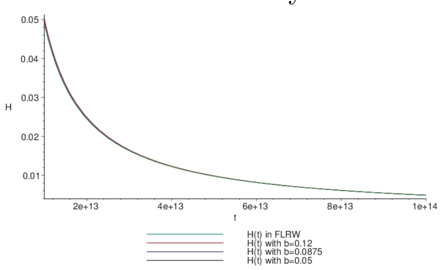

(c) $H(t)$ [km/s/Mpc] in the range of $10^{13} - 10^{14}$ years

Figure 19: F as a nodal sink with $c_1 = 0$ and $c_2 = 1$: H(t) for different values of β and $w = 1/3$ which represents radiation.

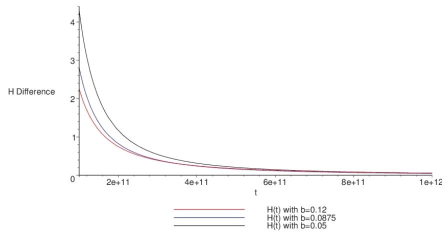

(a) Difference of $H(t)$ [km/s/Mpc] in the range of $10^{11} - 10^{12}$ years

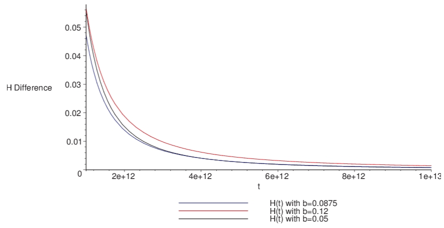

(b) Difference of $H(t)$ [km/s/Mpc] in the range of $10^{12} - 10^{13}$ years

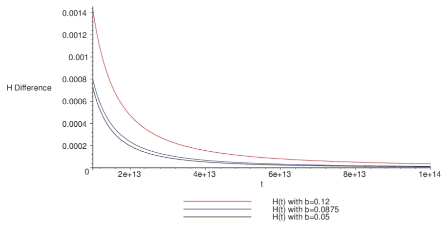

(c) Difference of $H(t)$ [km/s/Mpc] in the range of $10^{13} - 10^{14}$ years

Figure 20: F as a nodal sink with $c_1 = 0$ and $c_2 = 1$: Difference of H(t) for different values of β and the $H(t)$ of the FLRW model for $w = 1/3$ which represents radiation.

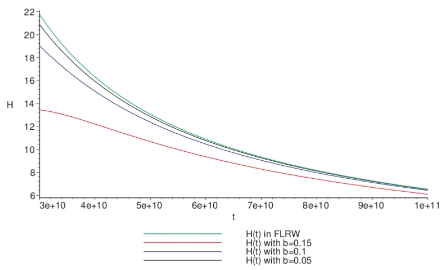

(a) $H(t)$ [km/s/Mpc] in the range of $3 \cdot 10^{10} - 10^{11}$ years

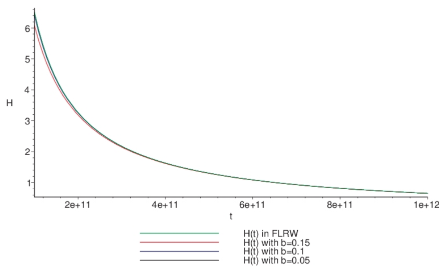

(b) $H(t)$ [km/s/Mpc] in the range of $10^{11} - 10^{12}$ years

Figure 21: F as a nodal sink with $c_1 = 0$ and $c_2 = 1$: H(t) for different values of β and $w = 0$ which represents dust.

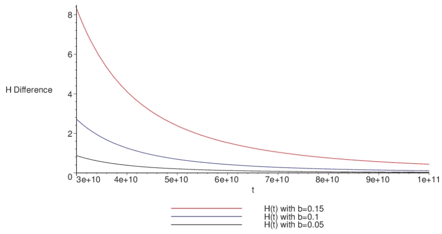

(a) Difference of $H(t)$ [km/s/Mpc] in the range of $3 \cdot 10^{10} - 10^{11}$ years

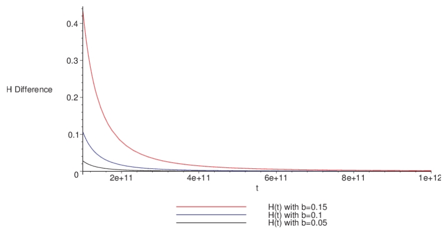

(b) Difference of $H(t)$ [km/s/Mpc] in the range of $10^{11} - 10^{12}$ years

Figure 22: F as a nodal sink with $c_1 = 0$ and $c_2 = 1$: Difference of H(t) for different values of β and the $H(t)$ of the FLRW model for $w = 0$ which represents dust.

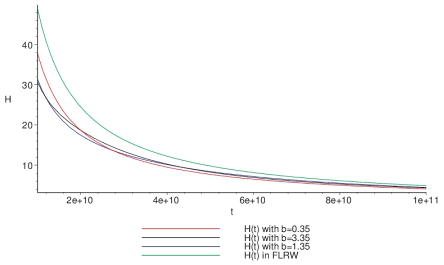

(a) $H(t)$ [km/s/Mpc] in the range of $10^{10} - 10^{11}$ years

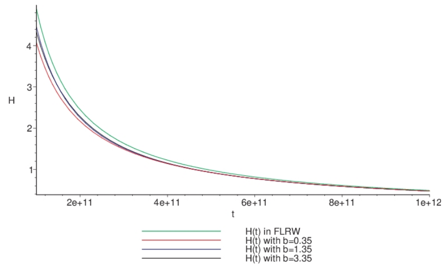

(b) $H(t)$ [km/s/Mpc] in the range of $10^{11} - 10^{12}$ years

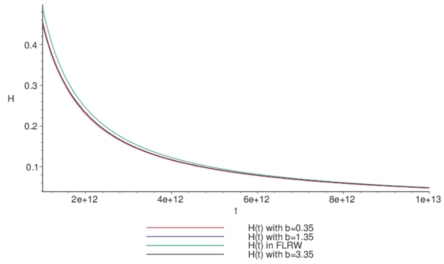

(c) $H(t)$ [km/s/Mpc] in the range of $10^{12} - 10^{13}$ years

Figure 23: F as a spiral sink with $c_1 = 1$ and $c_2 = 0$: $H(t)$ for different values of β and $w = 1/3$ which represents radiation.

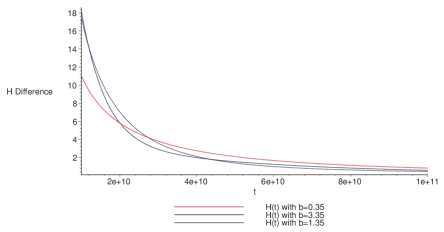

(a) Difference of $H(t)$ [km/s/Mpc] in the range of $10^{10} - 10^{11}$ years

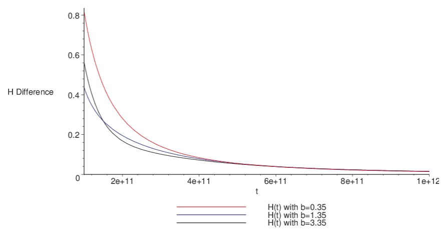

(b) Difference $H(t)$ [km/s/Mpc] in the range of $10^{11} - 10^{12}$ years

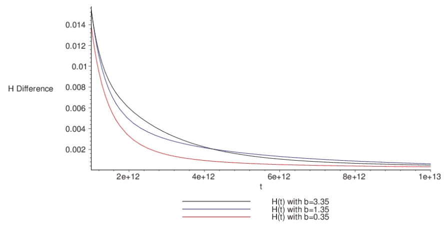

(c) Difference $H(t)$ [km/s/Mpc] in the range of $10^{12} - 10^{13}$ years

Figure 24: F as a spiral sink with $c_1 = 1$ and $c_2 = 0$: Difference of $H(t)$ for different values of β and $H(t)$ of the FLRW model for $w = 1/3$ which represents radiation.

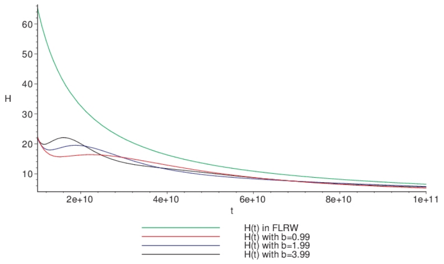

(a) $H(t)$ [km/s/Mpc] in the range of $10^{10} - 10^{11}$ years

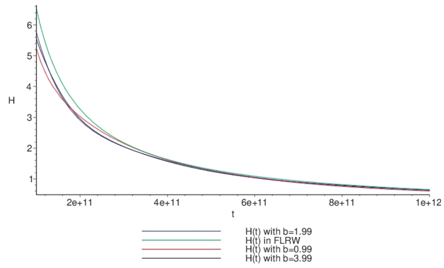

(b) $H(t)$ [km/s/Mpc] in the range of $10^{11} - 10^{12}$ years

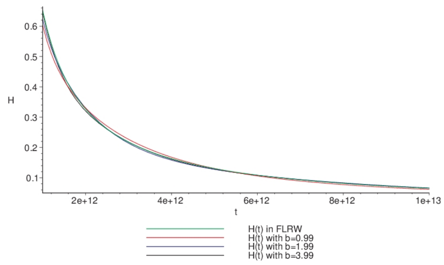

(c) $H(t)$ [km/s/Mpc] in the range of $10^{12} - 10^{13}$ years

Figure 25: F as a spiral sink with $c_1 = 1$ and $c_2 = 0$: $H(t)$ for different values of β and $w = 0$ which represents dust.

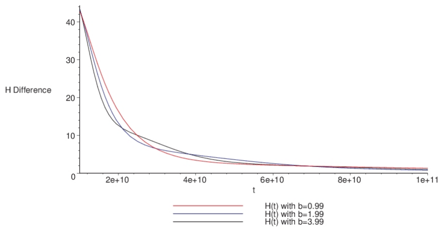

(a) Difference of $H(t)$ [km/s/Mpc] in the range of $10^{10} - 10^{11}$ years

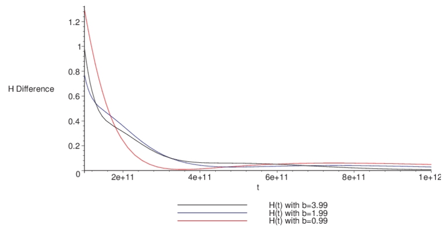

(b) Difference of $H(t)$ [km/s/Mpc] in the range of $10^{11} - 10^{12}$ years

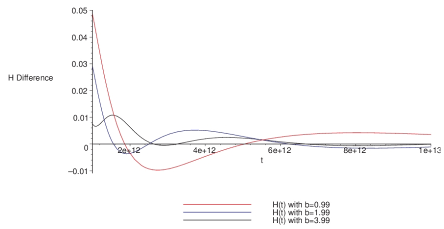

(c) Difference of $H(t)$ [km/s/Mpc] in the range of $10^{12} - 10^{13}$ years

Figure 26: F as a spiral sink with $c_1 = 1$ and $c_2 = 0$: Difference of $H(t)$ for different values of β and $H(t)$ of the FLRW model for $w = 0$ which represents radiation.

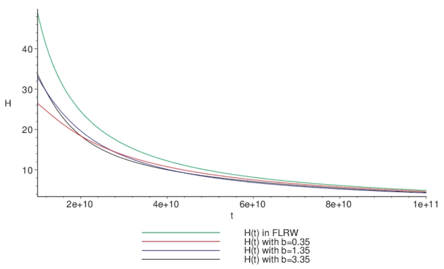

(a) $H(t)$ [km/s/Mpc] in the range of $10^{10} - 10^{11}$ years

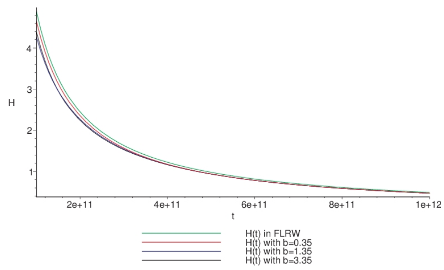

(b) $H(t)$ [km/s/Mpc] in the range of $10^{11} - 10^{12}$ years

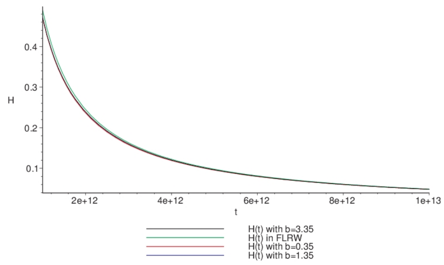

(c) $H(t)$ [km/s/Mpc] in the range of $10^{12} - 10^{13}$ years

Figure 27: F as a spiral sink with $c_1 = 0$ and $c_2 = 1$: $H(t)$ for different values of β and $w = 1/3$ which represents radiation.

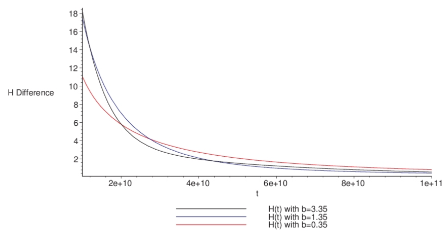

(a) Difference of $H(t)$ [km/s/Mpc] in the range of $10^{10} - 10^{11}$ years

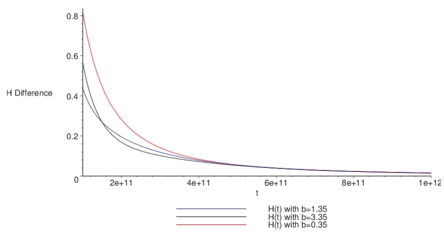

(b) Differnce of $H(t)$ [km/s/Mpc] in the range of $10^{11} - 10^{12}$ years

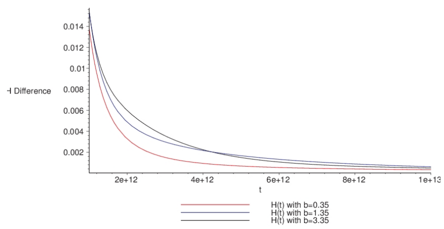

(c) Difference of $H(t)$ [km/s/Mpc] in the range of $10^{12} - 10^{13}$ years

Figure 28: F as a spiral sink with $c_1 = 0$ and $c_2 = 1$: Difference of $H(t)$ for different values of β and $H(t)$ of the FLRW model for $w = 1/3$ which represents radiation.

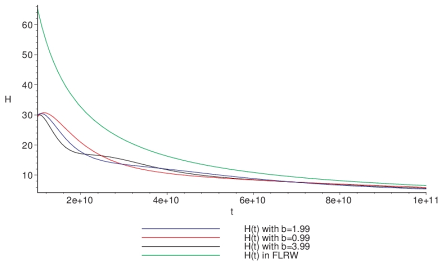

(a) $H(t)$ [km/s/Mpc] in the range of $10^{10} - 10^{11}$ years

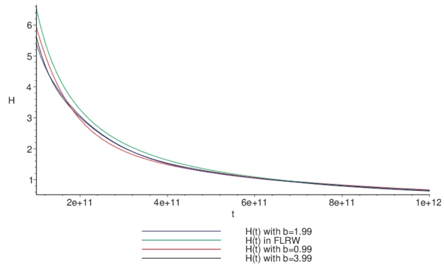

(b) $H(t)$ [km/s/Mpc] in the range of $10^{11} - 10^{12}$ years

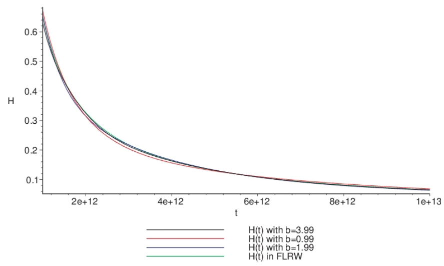

(c) $H(t)$ [km/s/Mpc] in the range of $10^{12} - 10^{13}$ years

Figure 29: F as a spiral sink with $c_1 = 0$ and $c_2 = 1$: $H(t)$ for different values of β and $w = 0$ which represents dust.

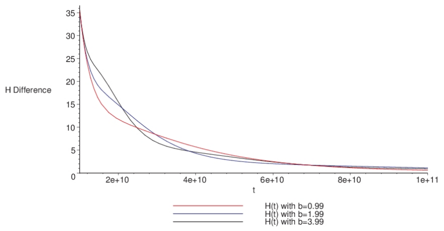

(a) Difference of $H(t)$ [km/s/Mpc] in the range of $10^{10} - 10^{11}$ years

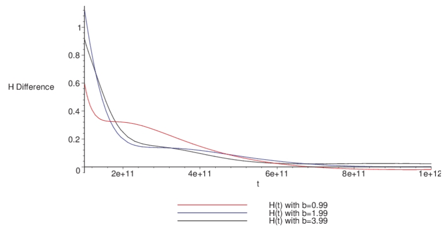

(b) Difference of $H(t)$ [km/s/Mpc] in the range of $10^{11} - 10^{12}$ years

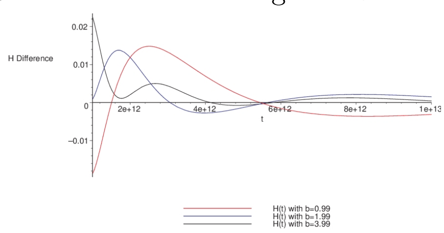

(c) Difference of $H(t)$ [km/s/Mpc] in the range of $10^{12} - 10^{13}$ years

Figure 30: F as a spiral sink with $c_1 = 0$ and $c_2 = 1$: Difference of $H(t)$ for different values of β and $H(t)$ of the FLRW model for $w = 0$ which represents radiation.

10 References

[1] Amann, H., Gewöhnliche Differentialgleichungen, de Gruyter Lehrbuch, 1983

[2] Baumgarte, T.W., Shapiro, S.L., Cambridge University Press, 2010

[3] Calogero, S., Heinzle, J.M., Asymptotics of LRS Bianchi type I cosmoligical models with elastic matter, General Relativity and Gravitation, Volume 42, Number 6, 2010

[4] Calogero, S., Heinzle, J.M., Bianchi Cosmologies with Anisotropic Matter: Locally Rotationally Symmetric Models, Physica D: Nonlinear Phenomena, Volume 240, Issue 7, 2011

[5] Carroll, M.S., The Cosmological Constant, Living Rev. Relativity, 3, (2001), 1

[6] Chaboyer, B., Absolute ages of globular clusters and the age of the universe, Astrophysical Journal Letters, 1994

[7] Clarke, S.; Leibniz, G. W., A collection of papers, which passed between the late learned Mr. Leibnitz, and Dr. Clarke, in the years 1715 and 1716 : relating to the principles of natural philosophy and religion ; with an appendix, to which are added, letters to Dr. Clarke concerning liberty and necessity ... Also remarks upon a book, entituled 'A philosophical enquiry concerning human liberty' , Knapton, 1717

[8] Einstein, A., Die Grundlage der allgemeinen Relativitätstheorie, Annalen der Physik, Vierte Folge, Band 49, Nummer 7, 1916

[9] Einstein, A., Über die vom Relativitätsprinzip geforderte Trägheit der Energie, Jahrbuch der Radioaktivität und Elektronik, 1907

[10] Freedman, W.L., Madore, B.F., Scowcroft, V., Burns, C., Monson, A., Persson, S.E., Seibert, M., A Mid-Infrared Calibration of the Hubble Constant, arXiv:1208.3281 [astro-ph.CO]

[11] Hawkins, E., et al., The 2dF Galaxy Redshift Survey: correlation functions, peculiar velocities and the matter density of the Universe, Monthly Notices of the Royal Astronomical Society 346:78, 2003

[12] Hubble, E., A relation between distance and radial velocity among extra-galactic nebulae, Proceedings of the National Academy of Science, vol.15, 1929

[13] Hubble, E., Humason, M. L., The Velocity-Distance Relation among Extra-Galactic Nebulae, Astrophysical Journal, vol. 74, p.43, 1931

[14] Humason, M. L., Mayall, N. U., Sandage, A. R., red shifts and magnitudes of extragalactic nebulae, Astronomical Journal, Vol. 61, p. 97-162, 1956

[15] Mach, E. , The sience of mechanics, translated by McCormack, T.J., 4th edition, The open cort publishing Co., 1919

[16] Maddox, S.J., Efstathiou, G., Sutherland, W.J., Loveday, J., Galaxy correlations on large scales, Monthly Notices of the Royal Astronomical Society, Vol. 242, 1990

[17] Maddox, S.J., Sutherland, W.J., Efstathiou, G., Loveday, J., The APM galaxy survey - I. APM measurements and star-galaxy separation, Monthly Notices of the Royal Astronomical Society, Vol. 243, 1990

[18] Maddox, S.J., Efstathiou, G., Sutherland, W.J., The APM Galaxy Survey - II. Photometric corrections, Monthly Notices of the Royal Astronomical Society, Vol. 246, 1990

[19] Misner,C.W., Thorne, K.S., Wheeler, J.A., Gravitation, W.H. Freeman and Company, 1973

[20] Michelson, A.A., Morley, E.W., On the relative motion of the earth and the luminiferous aether, Philosophical Magazine and Journal of Science, Dec. 1887

[21] Newton, I., Philosophiæ Naturalis Principia Mathematica, S. PEPYS Reg. Soc. PRÆSES, 1686

[22] Newton, I., Newton's Principia, translated by A. Motte, published by D. Adee, University of California, 1846

[23] Patridge,R.B., Wilkinson, D.T., Isotropy and Homogeneity of the Universe from Measurements of the Cosmic Microwave Background, Phys. Rev. Lett. 18, 557-559, 1967

[24] Perko, L., Differential equations and dynamical systems. Springer, New York, 2001

[25] Reinhard, H., Differential equations - foundations and applications, translated by Howie, A., North Oxford Academic Publishers Ltd, 1986

[26] Rouche, N., Mawhin, J., Ordinary differential equations: stability and periodic solutions, Pitman Advanced Pub. Program, 1980

[27] Sandage, A., Current Problems in the Extragalactic Distance Scale, Astrophysical Journal, vol. 127, p.513

[28] Teschl, G., Ordinary Differential Equations and Dynamical Systems, Graduate Studies in Mathematics, 2012

[29] Wald, R.M., General Relativity, The University of Chicago, 1984

[30] Walter, W., Ordinary Differential Equations, Springer, 1998

[31] Warner, F.W. , Foundations of Differentiable Manifolds and Lie Groups, Graduate Texts in Mathematics 94, Springer, 1983

[32] Weinberg, S., Gravitation and Cosmology, John Wiley and Sons, 1972

11 Curriculum Vitae

Personal Data

Name:	Bettina WUTZL
Academic title:	Bachelor of Science (B.Sc.), Bakkelaurea der Naturwissenschaften (Bakk.rer.nat.)
Nationality:	Austria
e-mail:	bettinawutzl@a1.net

Education

Spring 2013	**Diploma thesis** in physics at the University of Vienna Thesis: Locally rotationally symmetric Bianchi type I cosmological models with anisotropic matter sources, supervisor: J.M. Heinzle
Since 2009	**Vienna University of Technology** Master Programme: Mathematics in Technology and Natural Science
October 2011	**Bachelor Degree of the University of Vienna**: Astronomy Thesis: Stellar Equilibrium and Collapse, supervisor: E. Dorfi
2008-2011	**University of Vienna** Bachelor Programme: Astronomy
September 2009	**Bachelor Degree of the Vienna University of Technology:** Mathematics in technology and natural science Thesis: Discussion of curves in the three dimensional Lorentz-Minkowski space, supervisor: F.Manhart
Summer Semester 09	**Semester abroad in Madrid** at the 'Universidad Complutense de Madrid' - Physics
2006-2009	**Vienna University of Technology** Bachelor Programme: Mathematics in Technology and Natural Science
Since 2006	**University of Vienna** Diploma Programme (Combined Bachelor and Master Programme): Physics
June 2006	**Matura:** School leaving examination at BRG/BORG in St.Pölten
2002-2006	**Secondary School:** BRG/BORG in St. Pölten (core area: Natural Science)

Work Experience

2008-2012	Tutor for the laboratory course 'Physics for Nutritionists' at the University of Vienna
July/August 2007	Assistant of the Local Authority
July/August 2007/06	Assistant of the Production at Constantia AG
August 2005	Assistant of the Quality Management at Constantia AG

Other skills

Language Skills: German (native), English (fluent), Spanish (fluent), Italian, French

Programming Skills: LaTeX, Maple, Matlab, GAMS, C, Python (Basics)

Spare Time

2005 to date	active member of the Landjugend
2012	onTOP certificate of the Landjugend (more than 25 hours in a training/educational event)
2010-2011	Press referent of the local Landjugend
2000-2006/ since 2011	Training in a dance studio and participant in several performances (e.g.Cats 2012)